Supporting Information

π-Stacked Dimerization of an Antiaromatic HomoHPHAC Monocation

Kaito Wada,[a] Yuma Tanioka,[a] Shigeki Mori,[b,c] Hidemitsu Uno[a] and Masayoshi Takase*[a,c]

[a] Graduate School of Science and Engineering, Ehime University, Matsuyama 790-8577, Japan
[b] Advanced Research Support Center (ADRES), Ehime University, Matsuyama 790-8577, Japan
[c] Research Unit on Molecular Materials Science for Toroidal π-Electron Systems, Ehime University, Matsuyama 790-8577, Japan

E-mail: takase.masayoshi.ry@ehime-u.ac.jp

Contents

General Information.

All reagents and solvents were of commercial reagent grade and were used without further purification except where noted. Unless otherwise noted, all reactions were performed with dry solvents under an atmosphere of nitrogen in dried glassware with standard vacuum-line techniques. All work-up and purification procedures were carried out with reagent-grade solvents in air. TLC analyses were performed on commercial Aluminium oxide 60 F_{254}, neutral (Merck). The developed chromatogram was analyzed by UV lamp (254 nm and 365 nm). Alumina column chromatography was performed on activated alumina (about 200 mesh) purchased from FUJIFILM Wako Pure Chemical Corporation. ^{1}H, ^{13}C and ^{19}F NMR spectra were recorded on a BRUKER AV500. Cyclic voltammetry (CV) measurements were performed on CH Instruments-ALS612B electrochemical analyzer using a standard three-electrode cell under nitrogen atmosphere. The potentials were calibrated with ferrocene as an external standard. Fast-atom bombardment (FAB) mass spectrum was measured on a JEOL JMS-700 instrument. LDI-TOF MS spectrum was measured on a JEOL JMS-S3000 at Ehime Institute of Industrial Technology. Absorption spectra were recorded on a JASCO V-570 spectrophotometer.

Synthetic procedures

***seco*DEHPHAC 2**

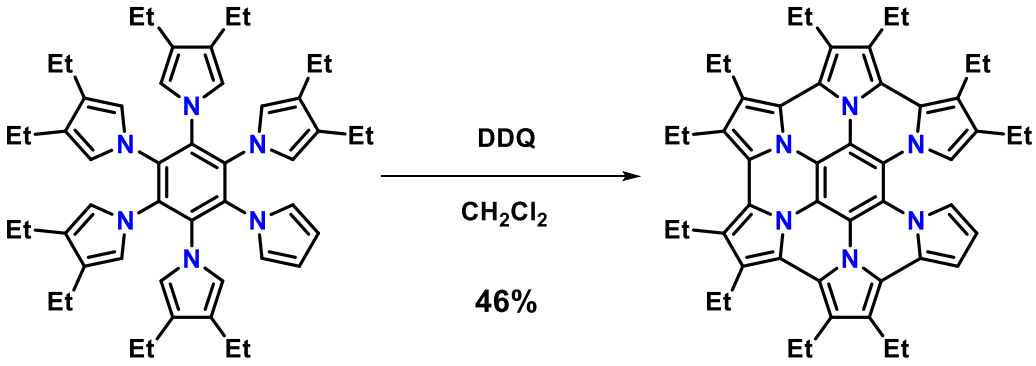

DEHPB 2

In a round-bottom flask, CH_2Cl_2 (400 mL) was added to a mixture of DEHPB (405.6 mg, 0.541 mmol) and DDQ (808.1 mg, 3.56 mmol) at 0 °C. The reaction mixture was stirred at room temperature for 2 days, then neutralized with hydrazine hydrate, and the solvent was removed under reduced pressure. The resulting solid was purified by alumina column chromatography (eluent: CH_2Cl_2) to give **2** as an orange solid. (185.7 mg, 0.251 mmol, 46%).

^{1}H NMR (500 MHz, chloroform-*d* in the presence of small amount of hydrazine hydrate and D_2O): δ 7.25 (m, 1H), 6.83 (s, 1H), 6.66 (m, 1H), 6.57 (m, 1H), 3.02-2.52 (m, 20H), 1.39-1.22 (m, 30H).

^{13}C NMR (126 MHz, chloroform-*d* in the presence of small amount of hydrazine hydrate and D_2O): δ 126.53, 124.53, 122.08, 121.60, 121.14, 121.11, 120.65, 120.56, 119.87, 119.68, 119.42, 118.11, 117.18, 116.41, 116.23, 115.98, 115.92, 115.82, 115.44, 114.92, 110.15, 109.33, 107.97, 107.63, 107.29, 107.23, 101.42, (Three kinds of carbon signals were overlapped in the range of 126.53-101.42 ppm), 17.62, 17.51, 17.47, 17.40, 17.34, 17.27, 17.25, 17.10, 16.41, 16.18, 16.13, 16.04, 15.63, 15.55, 15.29, 14.44, 14.14, 13.35. (Two kinds of carbon signals were overlapped in the range of 17.62-13.35 ppm).

HR MS (LDI): *m/z*: $[M]^+$ calcd. for $C_{50}H_{54}N_6$: 738.4404; found 738.4452.

mp > 140 °C (decomp.).

Antiaromatic homoHPHAC 3

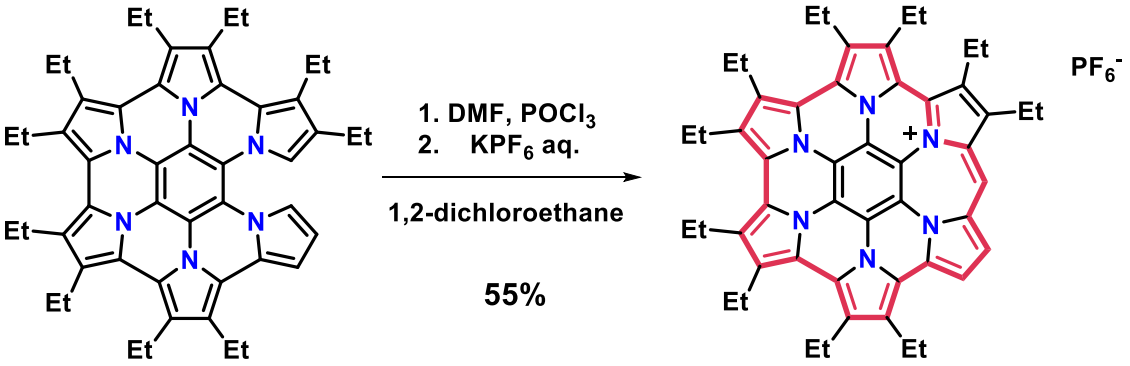

2 **3**

To a solution of DMF (0.4 mL, 5.2 mmol), $POCl_3$ (0.1 mL, 1.1 mmol) was added at room temperature. After stirring for 20 min, a solution of compound **2** (80.1 mg, 0.108 mmol) in 1,2-dichloroethane (2.0 mL) was added. The reaction mixture was stirred for an additional 15 h at 40 °C. The reaction was quenched by addition of $NaHCO_3$ aq. and the aqueous layer was extracted with EtOAc. The combined organic layers were washed successively with $NaHCO_3$ aq., water, and KPF_6 aq., and the solvent was removed under reduced pressure. The resulting solid was purified by alumina column chromatography (eluent: CH_2Cl_2/EtOAc = 20:1) to give **3** as a dark brown powder. (45.9 mg, 0.0513 mmol as PF_6 salt, 55%).

^{1}H NMR (500 MHz, acetone-d_6): δ 5.44 (d, J = 4.8 Hz, 1H), 5.32 (d, J = 4.7 Hz, 1H), 4.18 (s, 1H), 2.10 (q, J = 7.2 Hz, 2H), 1.80 (q, J = 7.1 Hz, 2H), 1.21-1.51 (m, 16H), 0.90 (t, J = 7.5 Hz, 3H), 0.80 (t, J = 7.5 Hz, 3H), 0.45-0.65 (m, 24H).

^{13}C NMR (126 MHz, acetone-d_6): δ 152.21, 147.83, 147.06, 138.94, 136.94, 136.78, 134.82, 133.75, 131.19, 130.69, 130.14, 129.38, 127.78, 127.67, 127.33, 126.94, 126.90, 126.54, 126.21, 125.95, 125.92, 125.78, 125.73, 125.36, 125.18, 124.15, 123.28, 122.96, 122.51, 121.22, 114.57, 17.69, 17.60, 17.47, 17.16, 17.12, 17.03, 16.54, 16.48, 16.37, 15.71, 15.38, 15.35, 15.11, 15.08, 14.86, 14.62, 13.80. (Three kinds of carbon signals were overlapped in the range of 17.69-13.80 ppm).

^{19}F NMR (470 MHz, acetone-d_6): δ –70.25 (d, $J_{P\text{-}F}$ = 711 Hz), –71.76 (d, $J_{P\text{-}F}$ = 711 Hz).

HR MS (LDI): *m/z*: $[M]^+$ calcd. for $C_{51}H_{53}N_6$: 749.4326; found 749.4325

mp > 200 °C (decomp.).

This compound was further confirmed by X-ray crystallography.

S1. ^{1}H, ^{13}C and ^{19}F NMR spectra

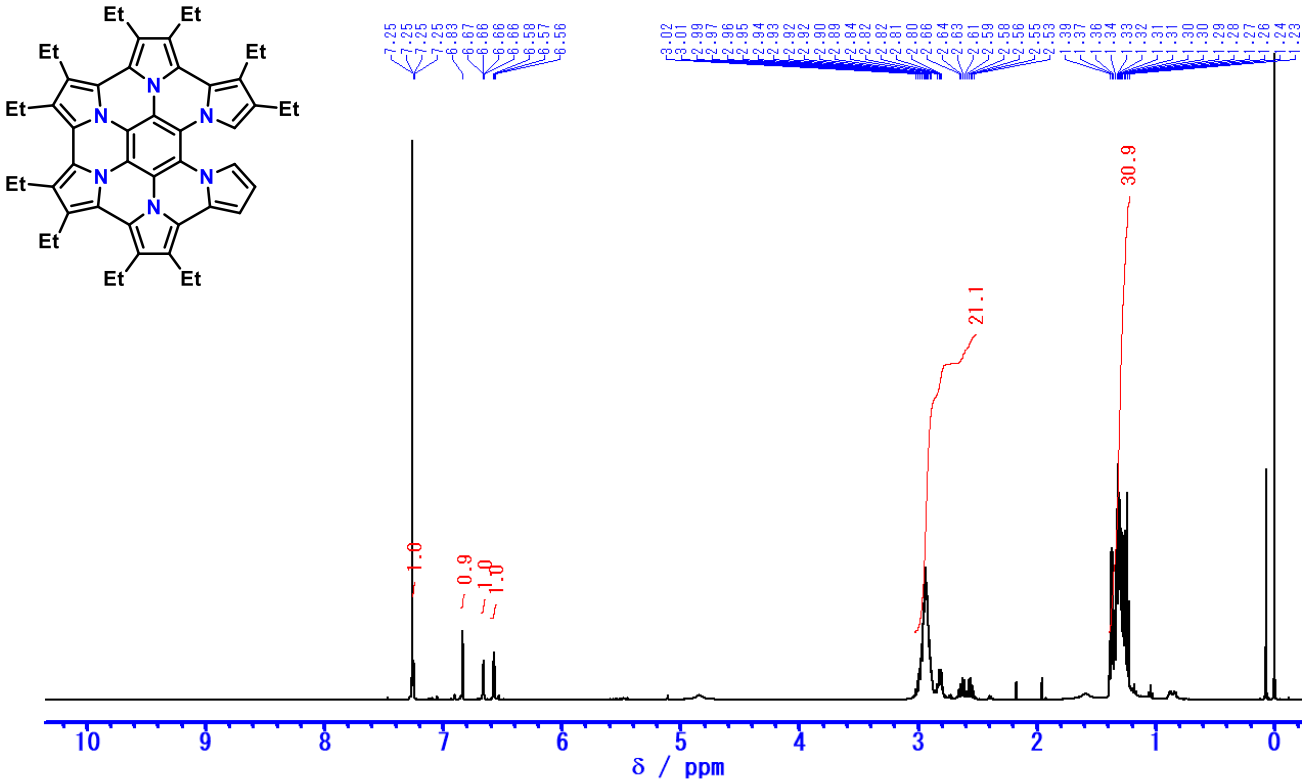

Figure S1a. ^{1}H NMR spectrum of **2** in chloroform-*d* in the presence of small amount of hydrazine hydrate and D_2O.

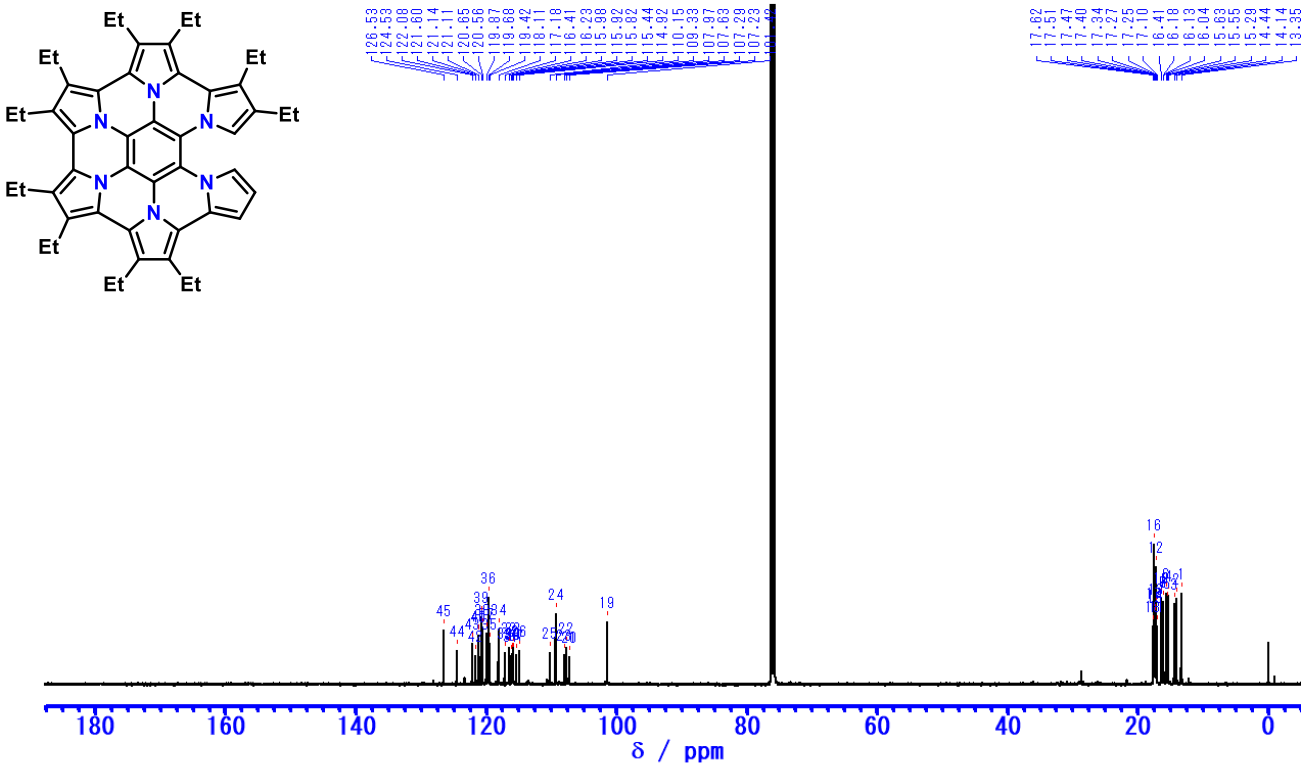

Figure S1b. ^{13}C NMR spectrum of **2** in chloroform-*d* in the presence of small amount of hydrazine hydrate and D_2O.

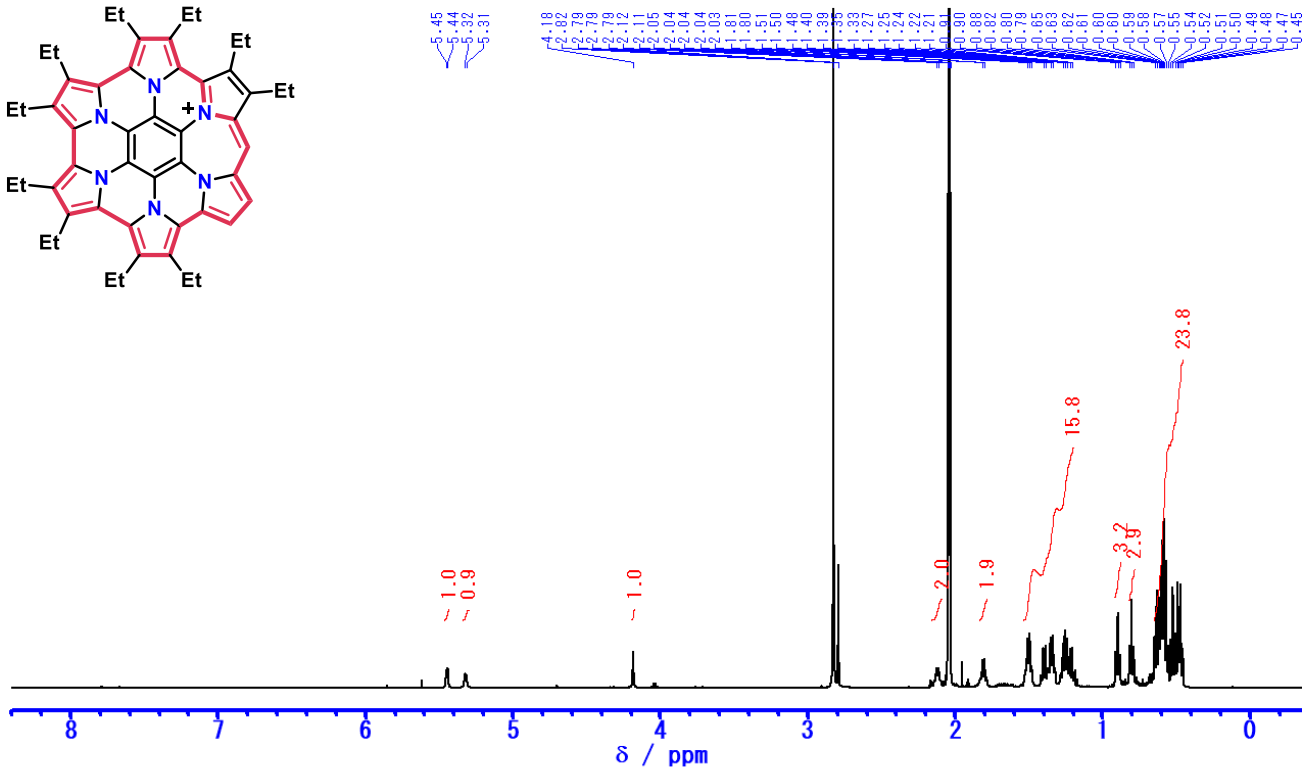

Figure S1c. ^{1}H NMR spectrum of **3** in acetone-d_6.

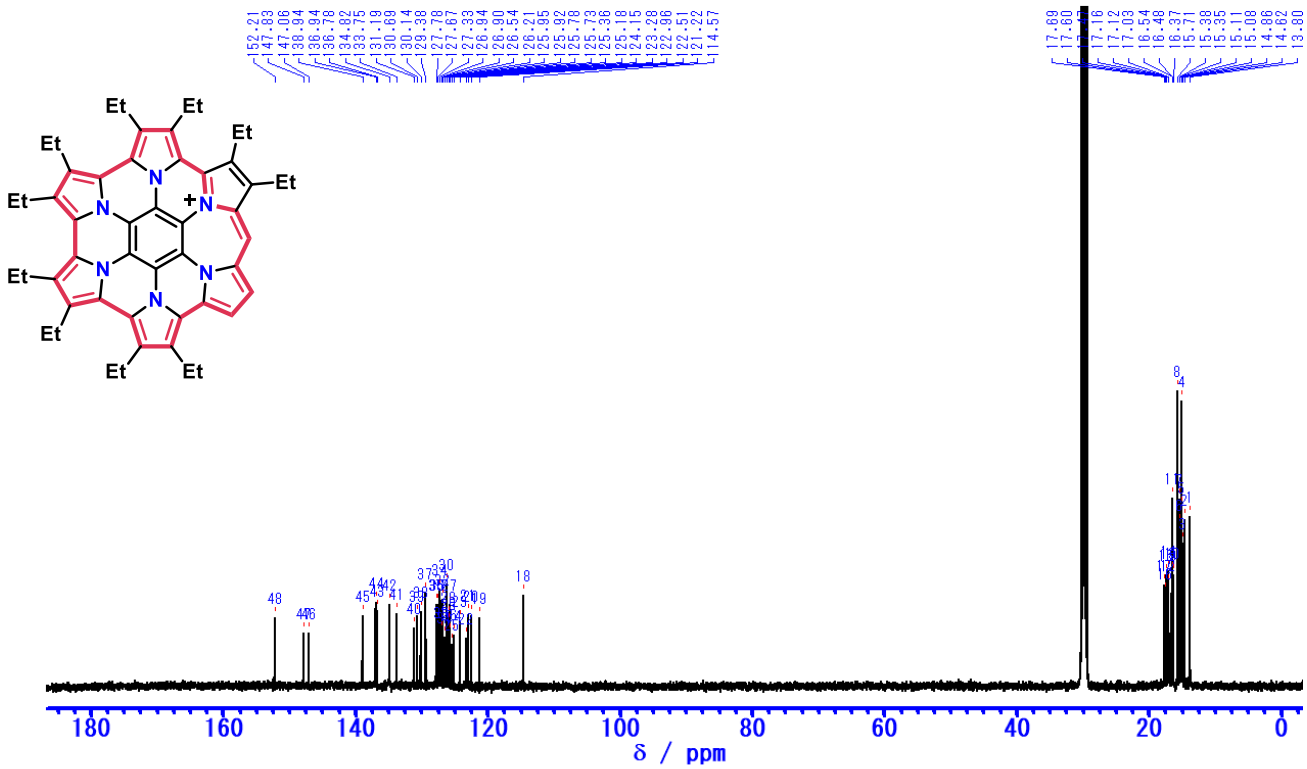

Figure S1d. ^{13}C NMR spectrum of **3** in acetone-d_6.

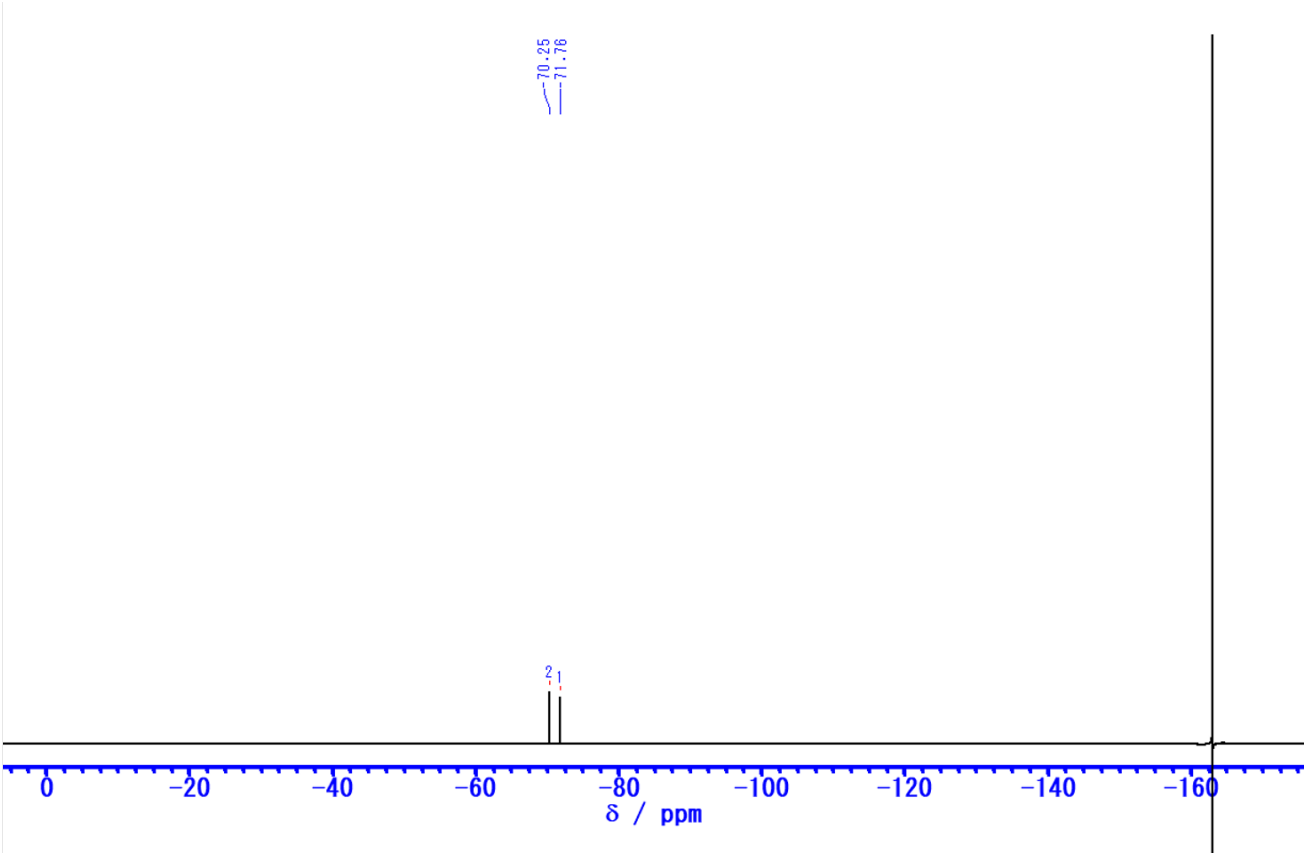

Figure S1e. ^{19}F NMR spectrum of **3** (PF_6 salt) in acetone-d_6 referenced to C_6F_6.

S2. NOESY spectra

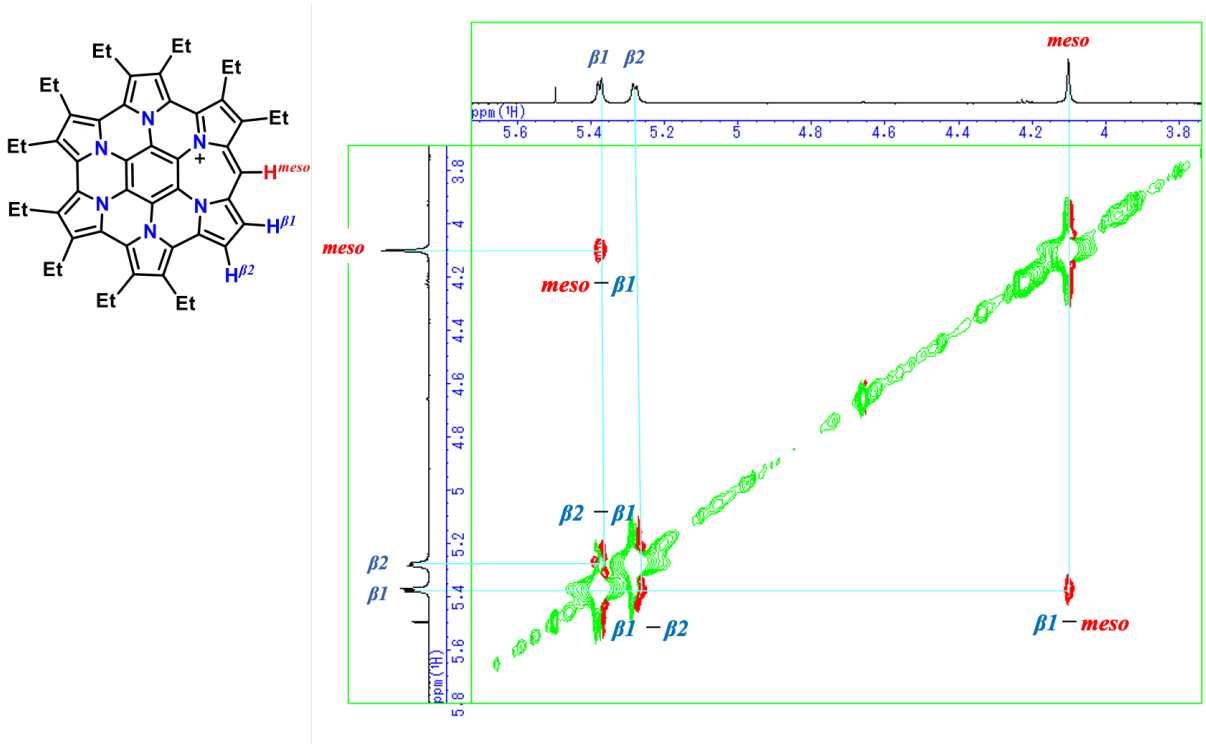

Figure S2a. NOESY spectrum of **3** in acetone-d_6 (the correlation between *meso* and β protons).

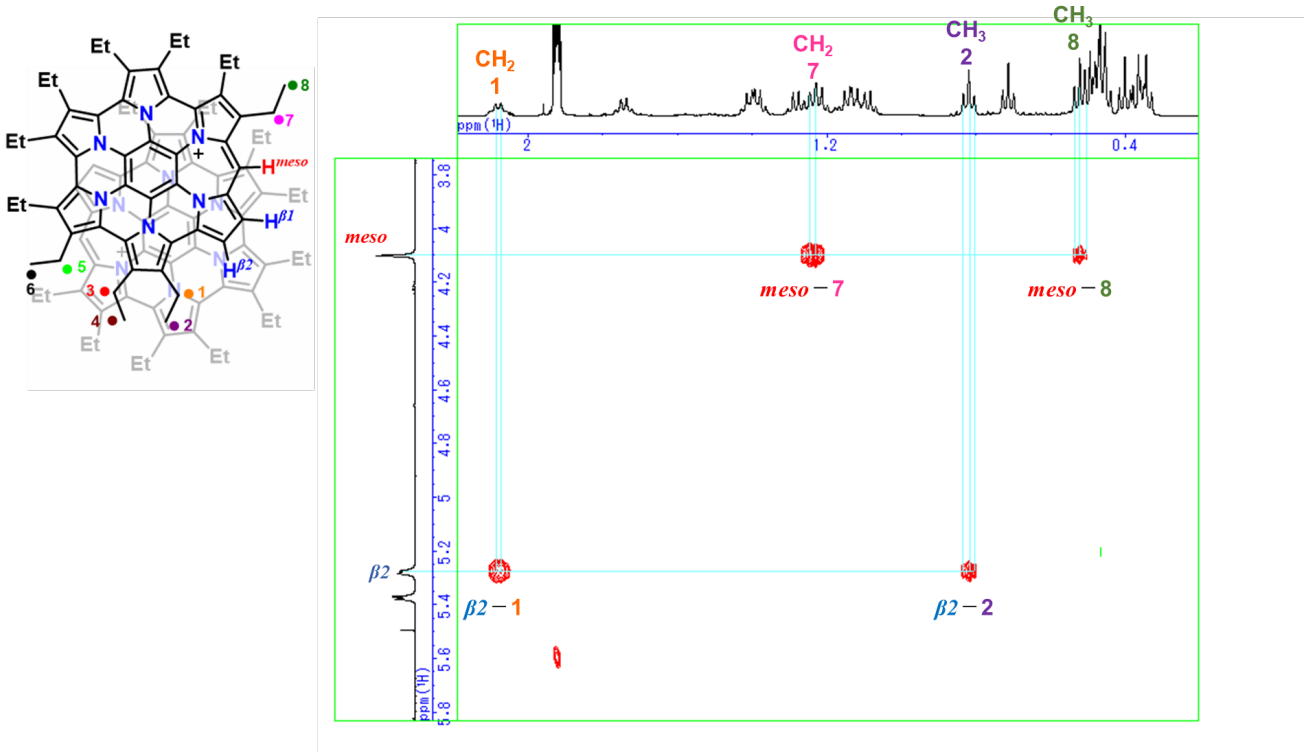

Figure S2b. NOESY spectrum of **3** in acetone-d_6 (the correlation between *meso*, β, and alkyl protons).

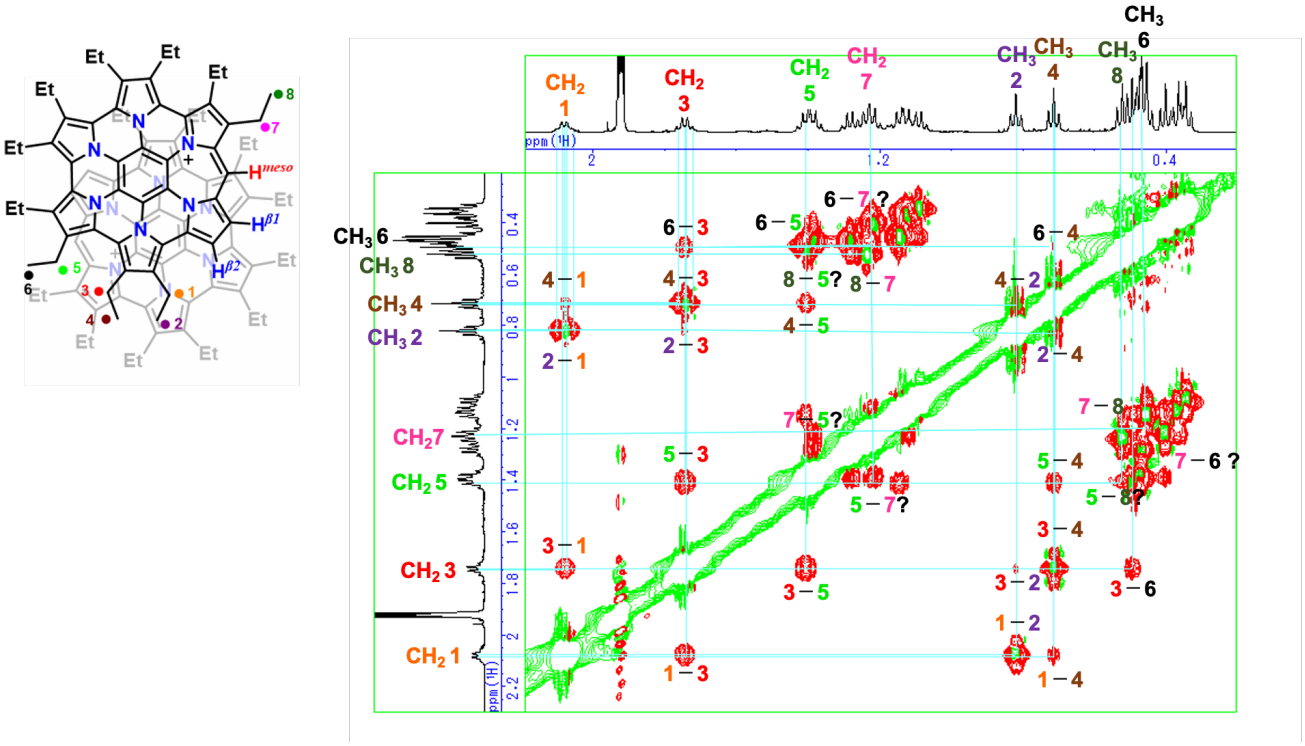

Figure S2c. NOESY spectrum of **3** in acetone-d_6 (the correlation of alkyl protons).

S3. ^{1}H & ^{19}F NMR spectra at various concentrations

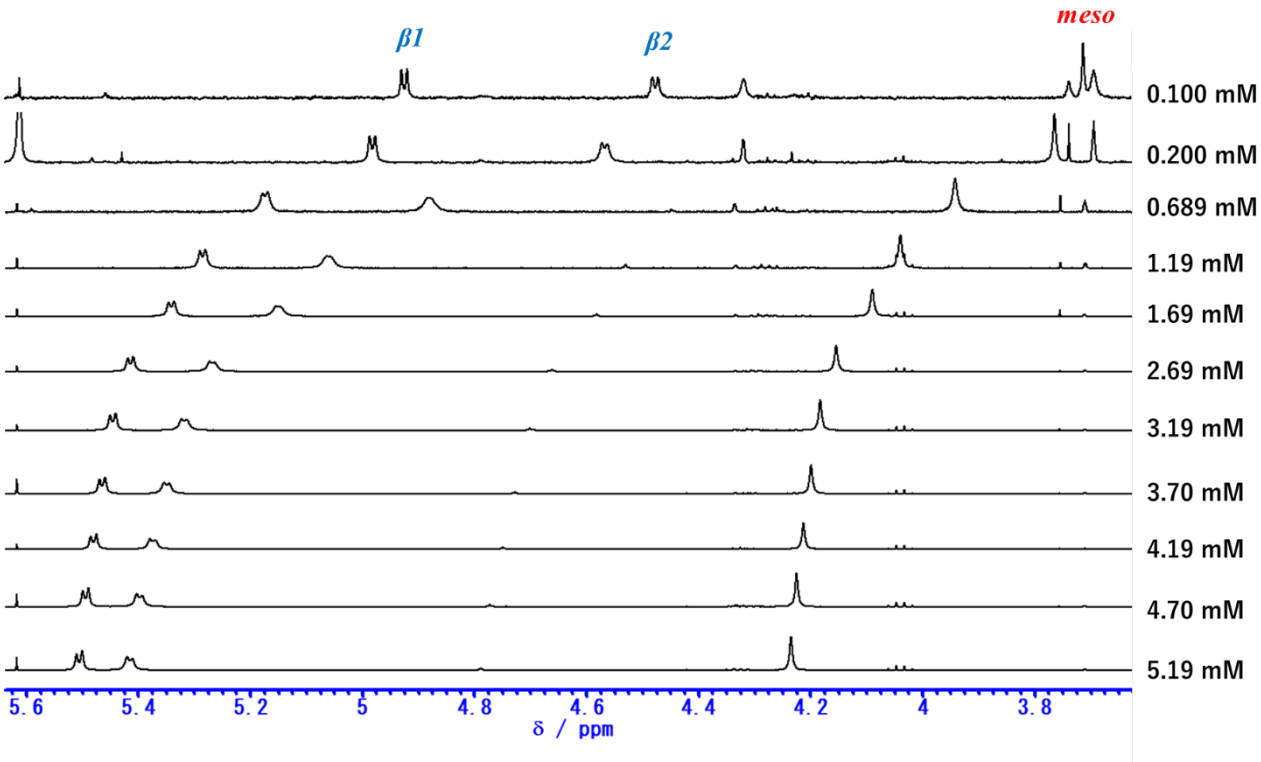

Figure S3a. ^{1}H NMR spectra of **3** in acetone-d_6 at 298 K.

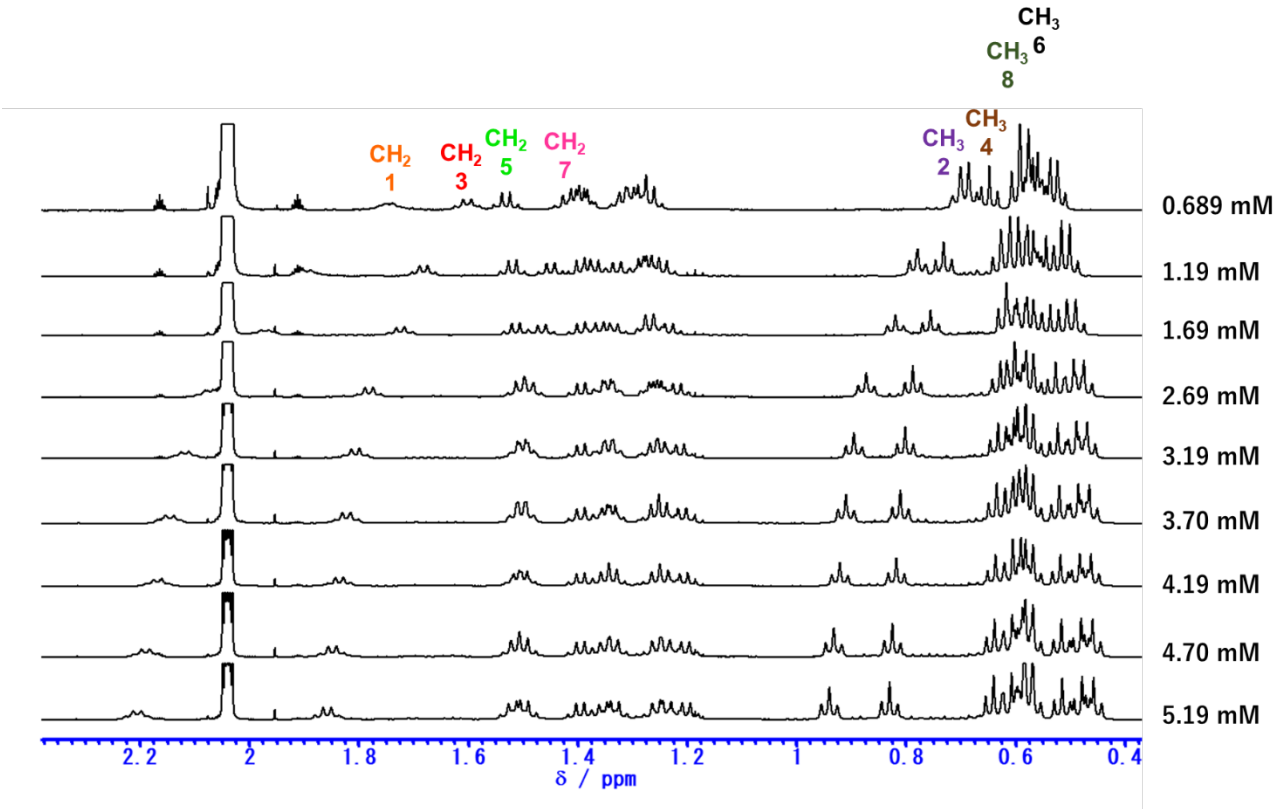

Figure S3b. ^{1}H NMR spectra of **3** in acetone-d_6 at 298 K (alkyl region).

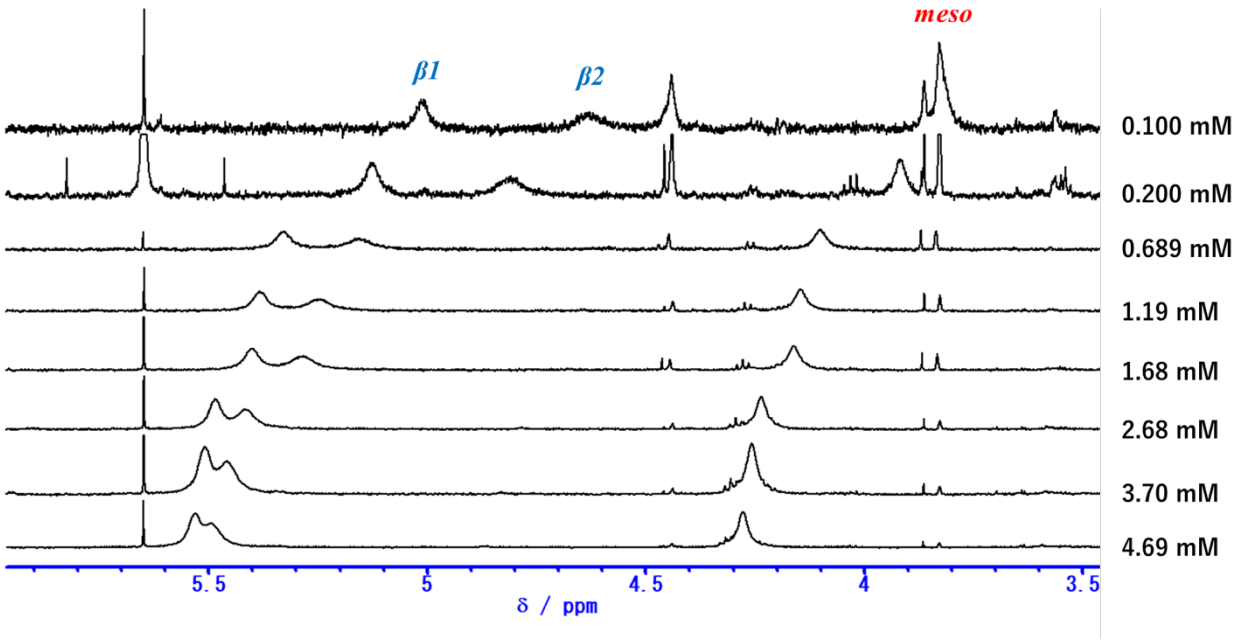

Figure S3c. ^{1}H NMR spectra of **3** in acetone-d_6 at 273 K.

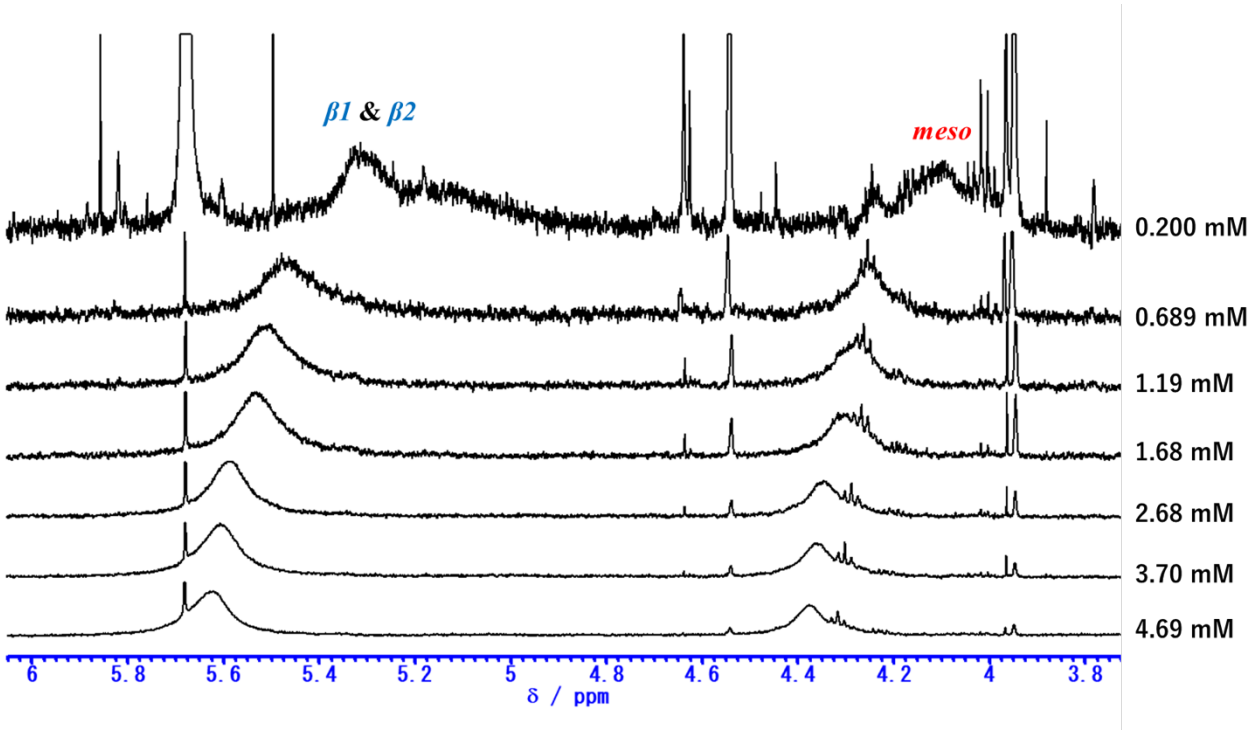

Figure S3d. ^{1}H NMR spectra of **3** in acetone-d_6 at 253 K.

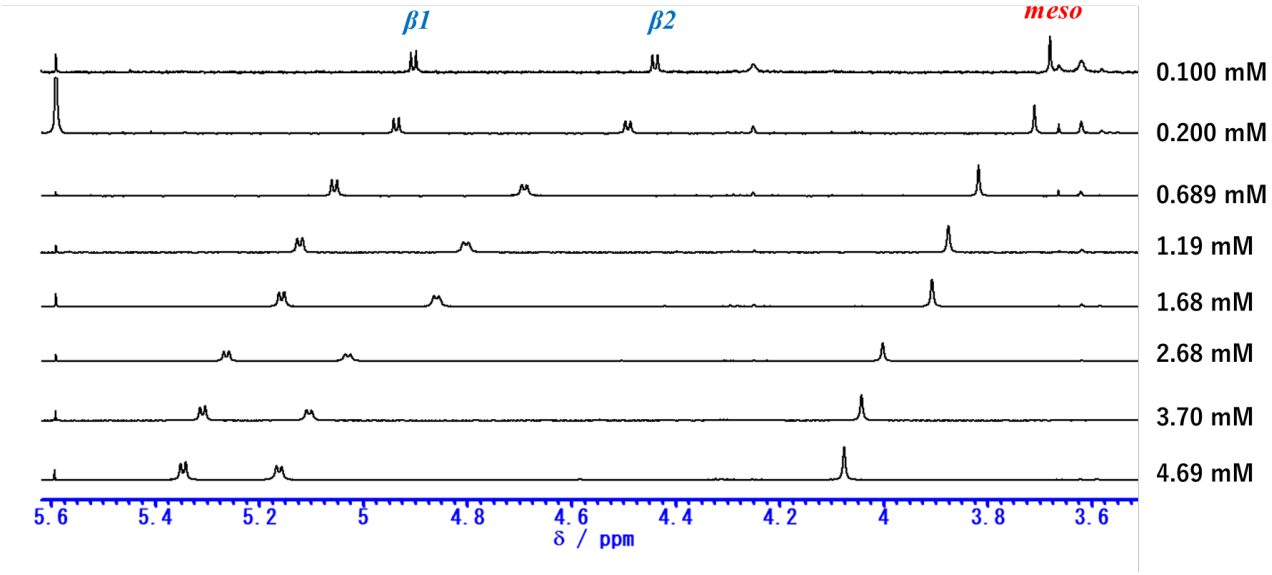

Figure S3e. ^{1}H NMR spectra of **3** in acetone-d_6 at 313 K.

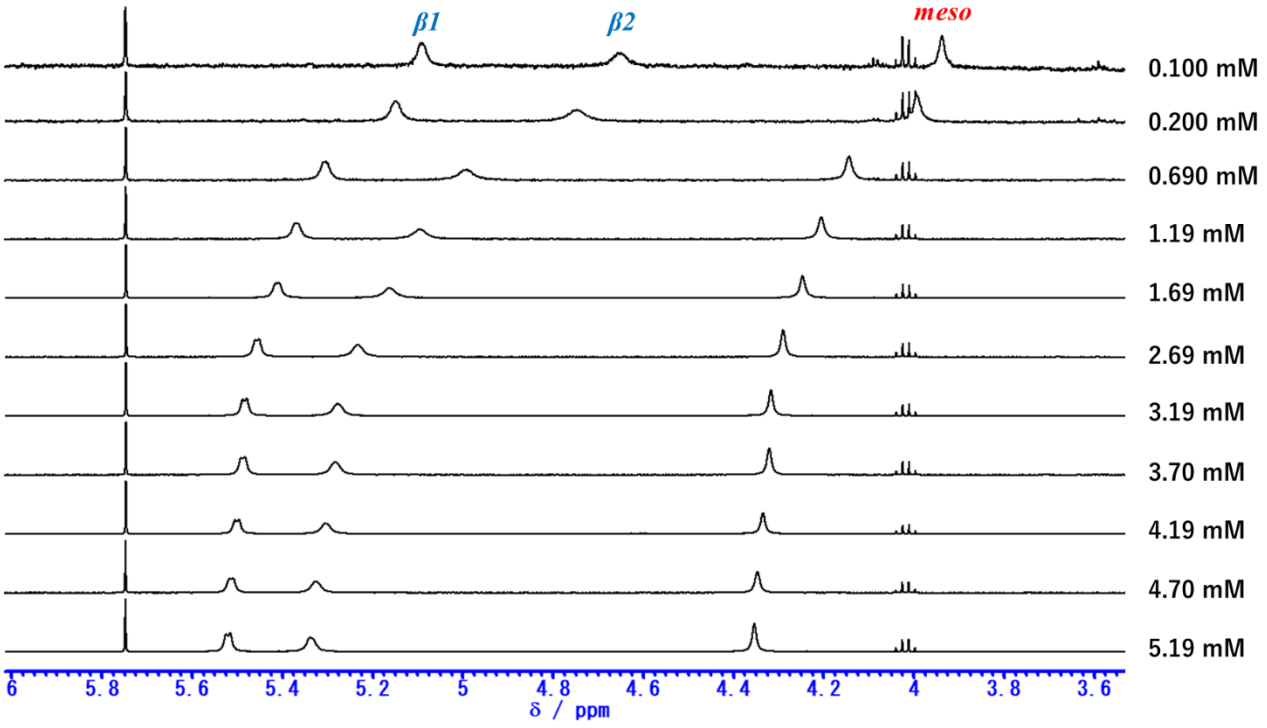

Figure S3f. ^{1}H NMR spectra of **3** in DMSO-d_6 at 298 K.

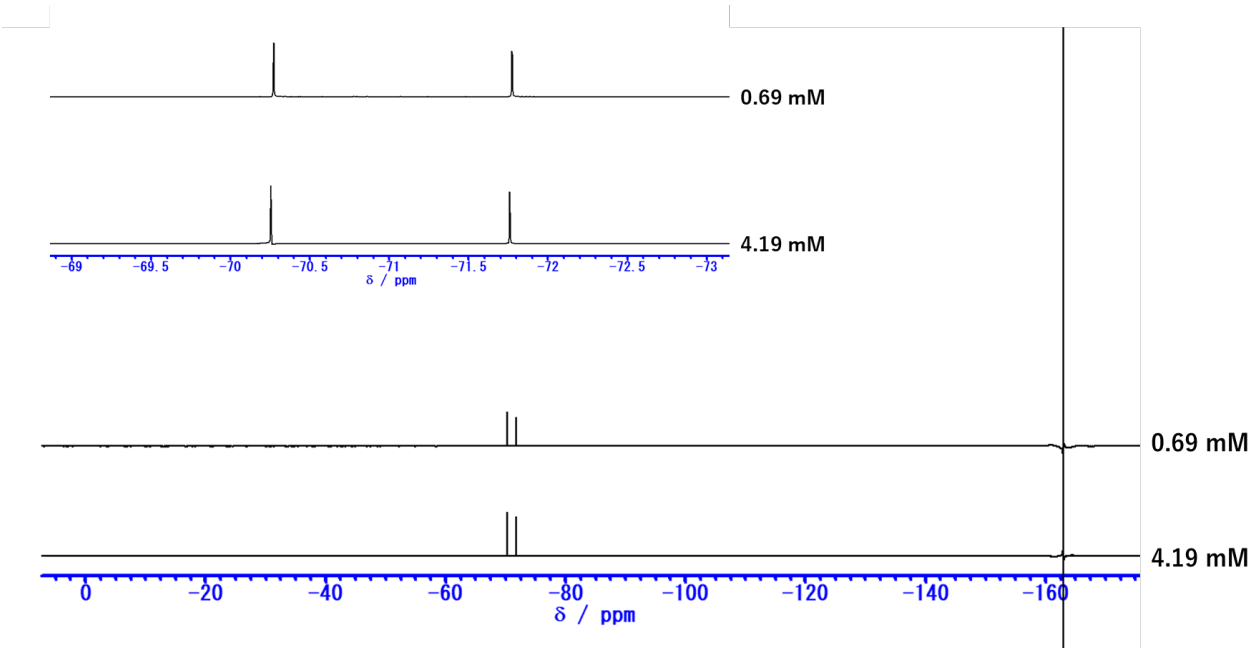

Figure S3g. ^{19}F NMR spectra of **3** in acetone-d_6 at 298 K.

S4. Nonlinear regression analysis of chemical shift changes

The equation (1)[1] with Curve fitting

$\delta = \delta_m + \{(\delta_d - \delta_m)(\sqrt{8KC_t + 1} - 1)\}/(\sqrt{8KC_t + 1} + 1)$ ····· (1)

(δ_m···The chemical shift value of monomer, δ_d···The chemical shift value of dimer, K···Association constant, C_t··· Concentration)

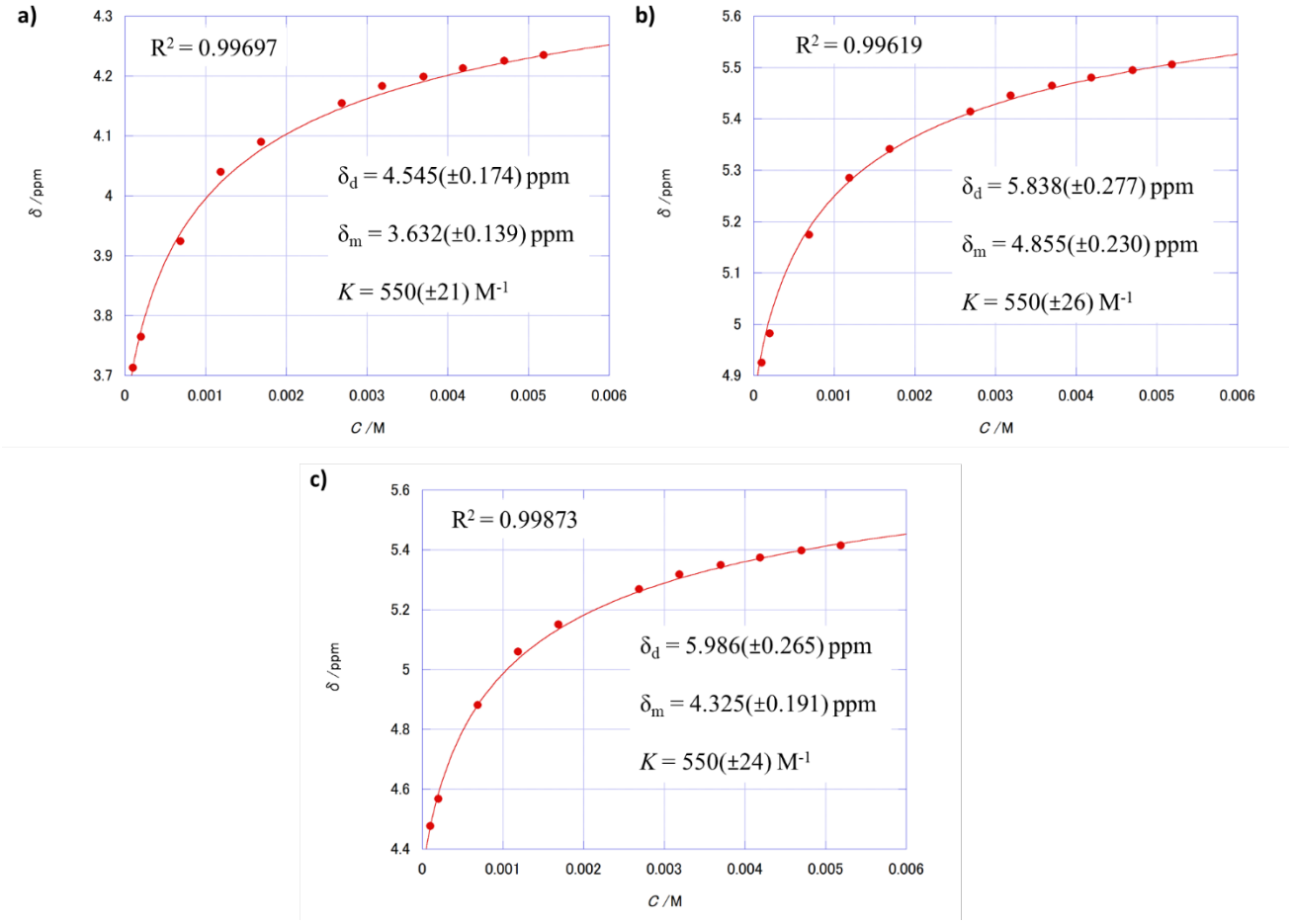

Figure S4a. Nonlinear curve regression analysis of the chemical shift changes of **3** (a) *meso*, (b) β 1 and (c) β 2 in acetone-d_6 at 298 K.

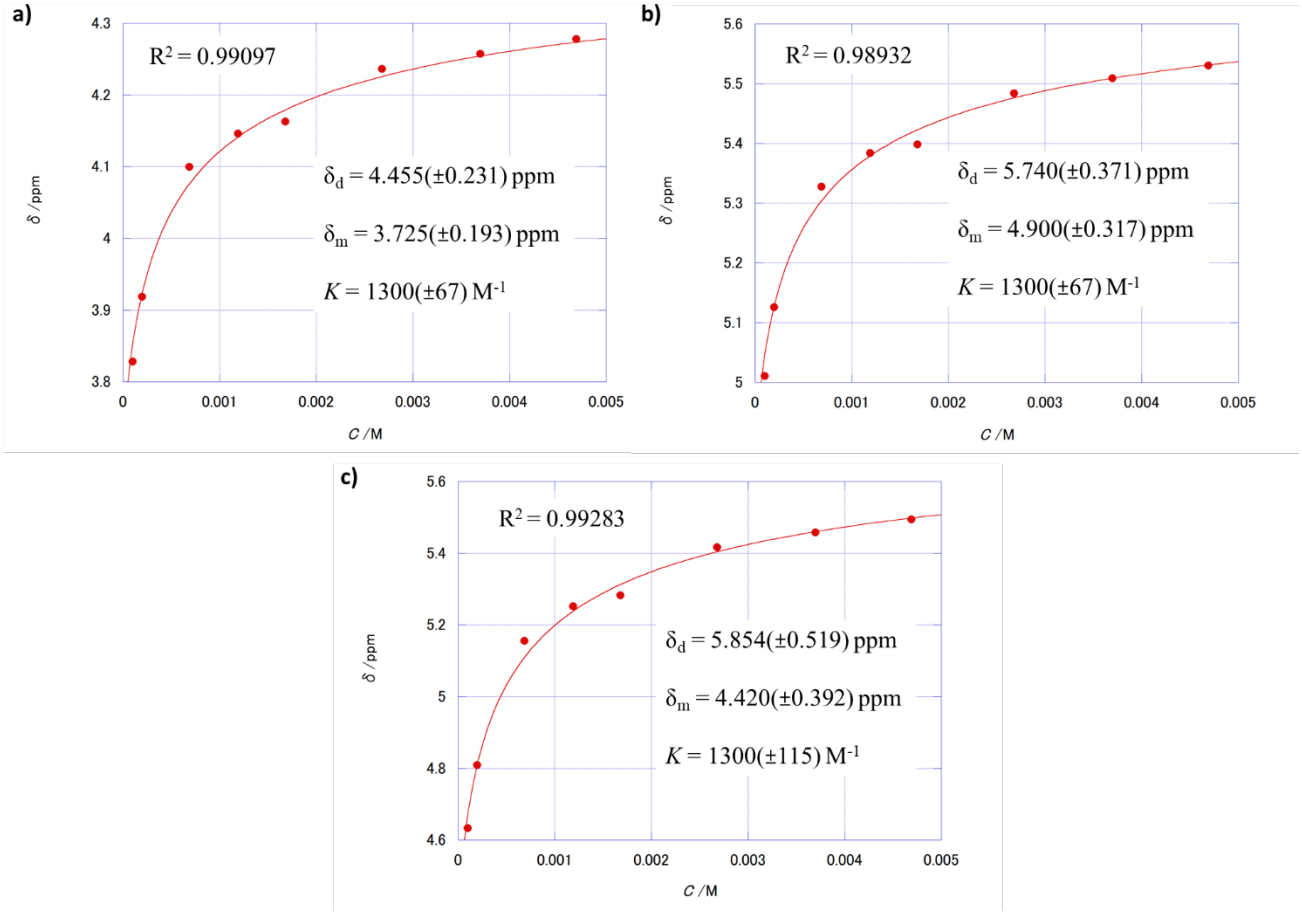

Figure S4b. Nonlinear curve regression analysis of the chemical shift changes of **3** (a) *meso*, (b) β 1 and (c) β 2 in acetone-d_6 at 273 K.

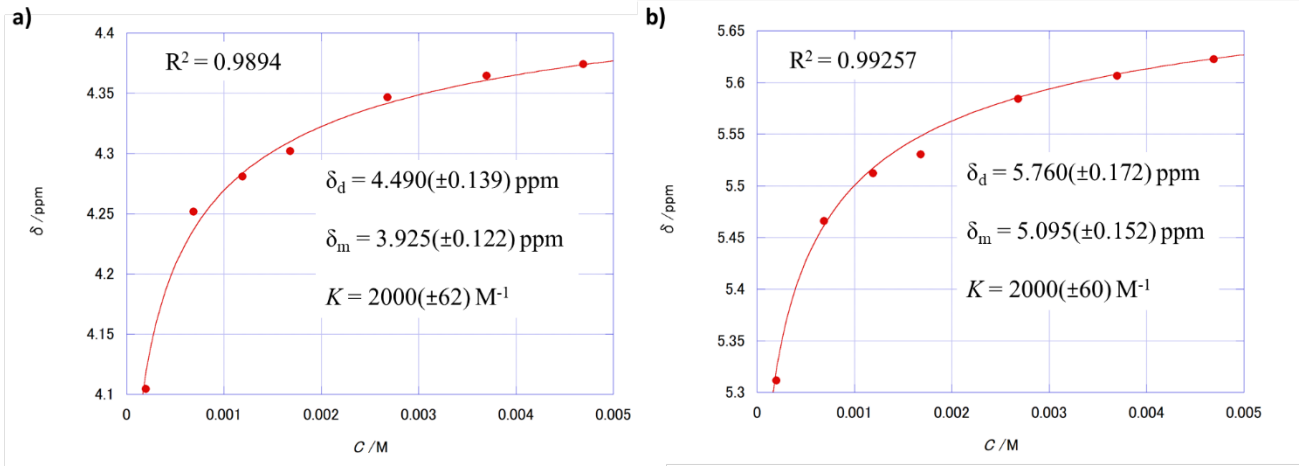

Figure S4c. Nonlinear curve regression analysis of the chemical shift changes of **3** (a) *meso* and (b) β in acetone-d_6 at 253 K.

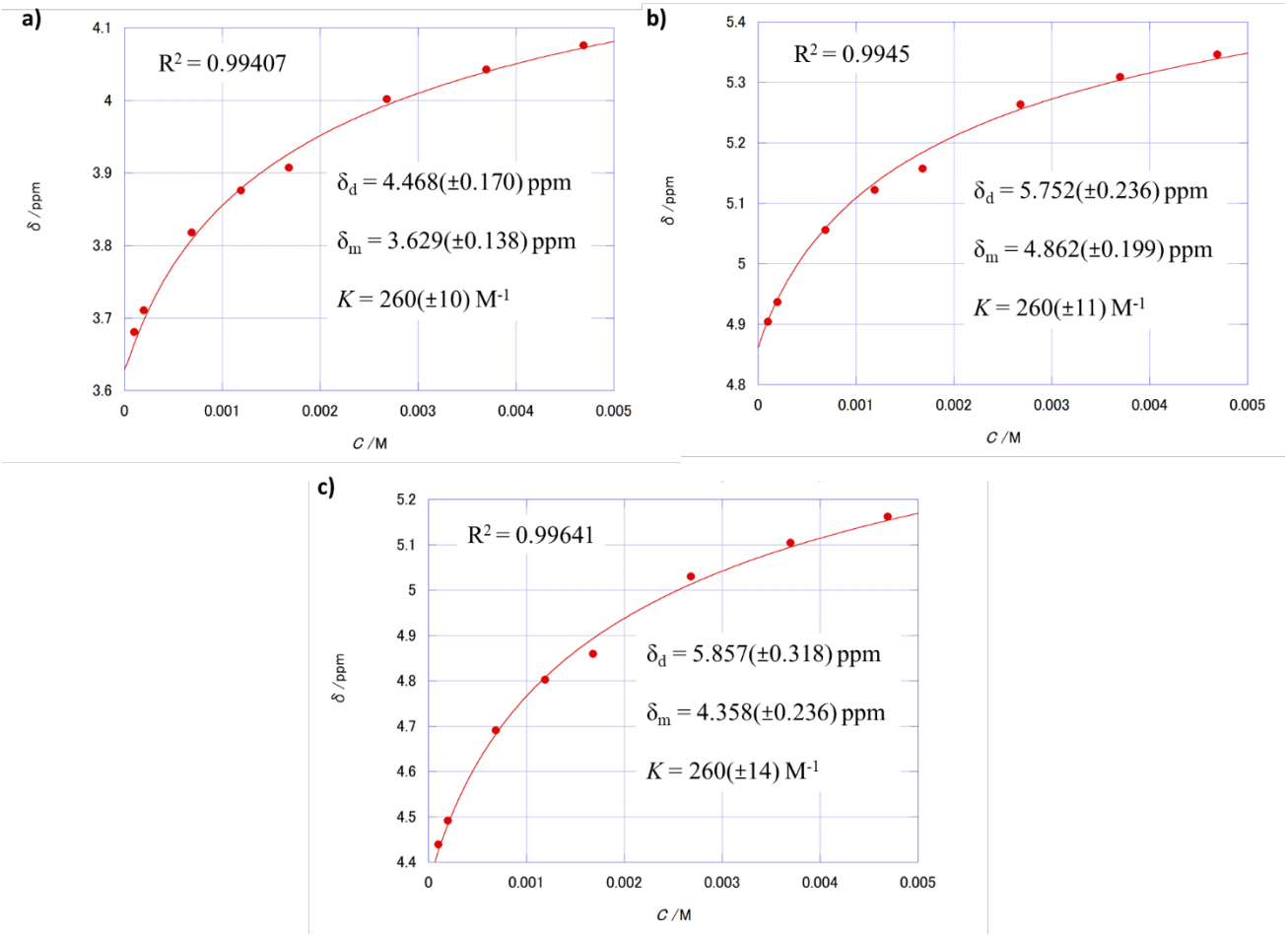

Figure S4d. Nonlinear curve regression analysis of the chemical shift changes of **3** (a) *meso*, (b) β 1 and (c) β 2 in acetone-d_6 at 313 K.

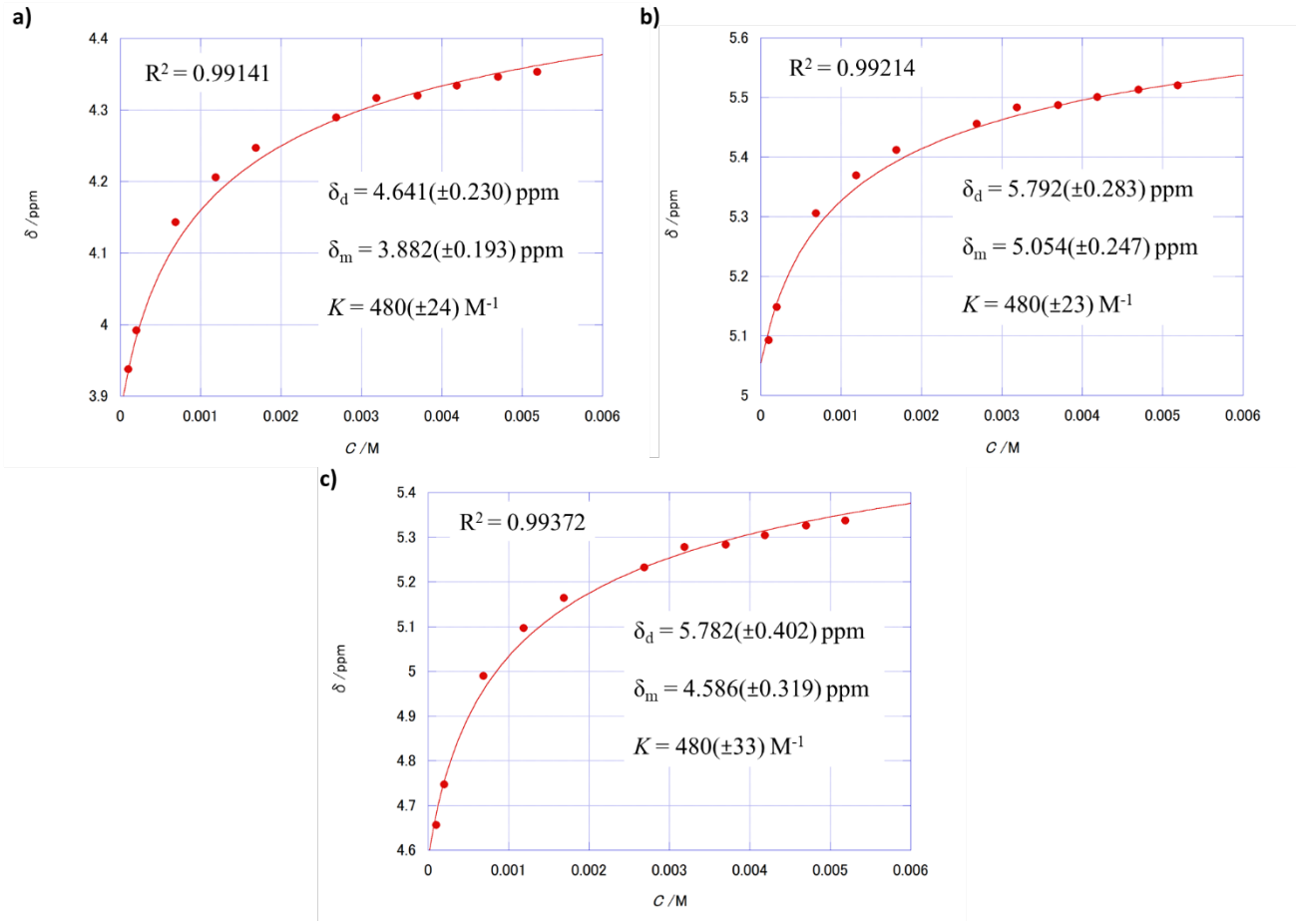

Figure S4e. Nonlinear curve regression analysis of the chemical shift changes of **3** (a) *meso*, (b) β 1 and (c) β 2 in DMSO-d_6 at 298 K.

Table S4. Association constants (K) of **3** in acetone-d_6 at various temperatures.

T [K]	K [M^{-1}]
253	2000
273	1300
298	550
313	260

S5. Thermodynamic parameters for equilibrium between monomer and dimer

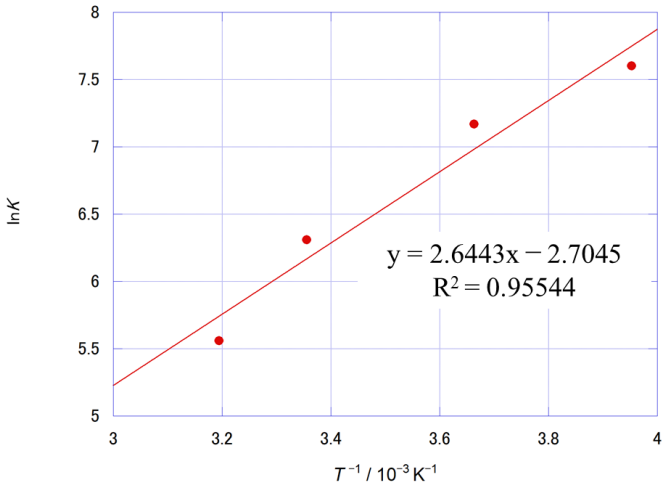

Figure S5. The van't Hoff plot of association constants (K) of **3** in acetone-d_6 at various temperatures.

Table S5. Thermodynamic parameters for equilibrium between monomer and dimer of **3** in acetone-d_6.

ΔG_{298} [kJ mol^{-1}]	ΔH [kJ mol^{-1}]	ΔS [J K^{-1} mol^{-1}]
−15.3	−22.0	−22.5

S6. High–resolution mass spectra

Exact mass: $C_{50}H_{54}N_6^+$; 738.4404

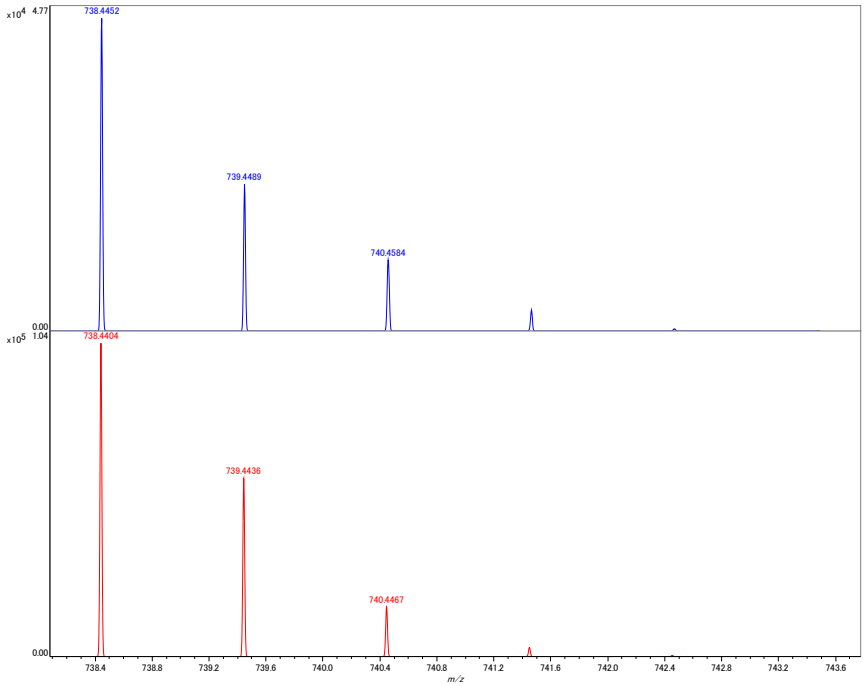

Figure S6a. High-resolution LDI-TOF MS spectrum of **2** (Top: observed, Bottom: simulated).

Exact mass: $C_{51}H_{53}N_6^+$; 749.4326

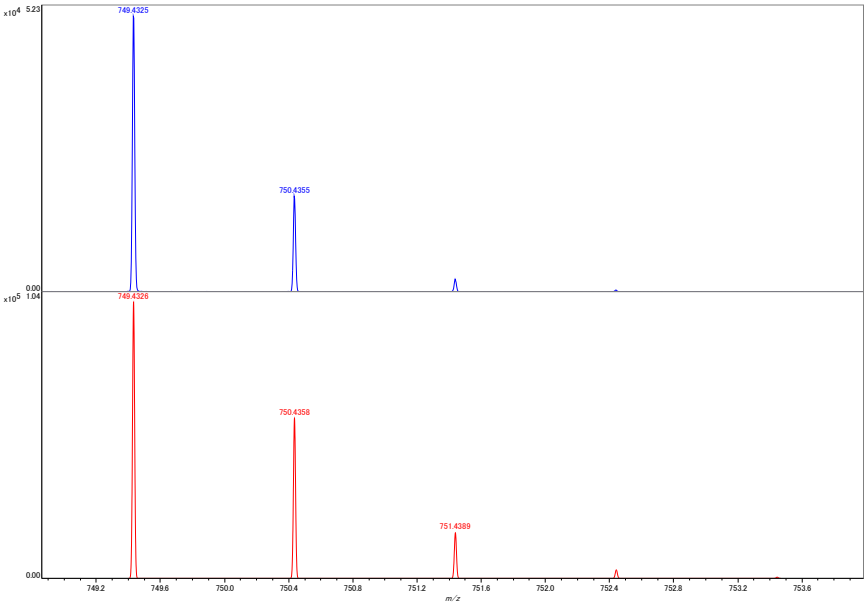

Figure S6b. High-resolution LDI-TOF MS spectrum of **3** (Top: observed, Bottom: simulated).

S7. X–ray crystal structure

Crystallographic analysis: X-ray diffraction analysis was performed using a Rigaku VariMax with Saturn diffractometer using multilayer mirror monochromated Mo Kα radiation (λ=0.71073 Å) at 100 K. The crystals were mounted in cryoloops. Data collection was performed using CrystalClear software. Data reduction was performed using RAPID AUTO or CrystalClear or CrysAlisPro software. The data were corrected for Lorentz polarization and absorption effects. The structures were solved using SHELXT 2014/5[2] and expanded using the Fourier technique. All calculations were performed using Rigaku Crystal-Structure crystallographic software package. SHELXL-2018/3[3] was used for structure refinement. The data were validated using PLATON.

One of the diethyl pyrrolic groups disordered. Consequently, the atomic coordinates and thermal parameters of the system were restrained by SADI, ISOR, RIGU, and SIMU commands. The counter-anion of SbF_6^- also disordered. The disordering of SbF_6^- was modelled as three components, and their atomic coordinates and thermal parameters were restrained by SADI, ISOR, RIGU, and SIMU commands.

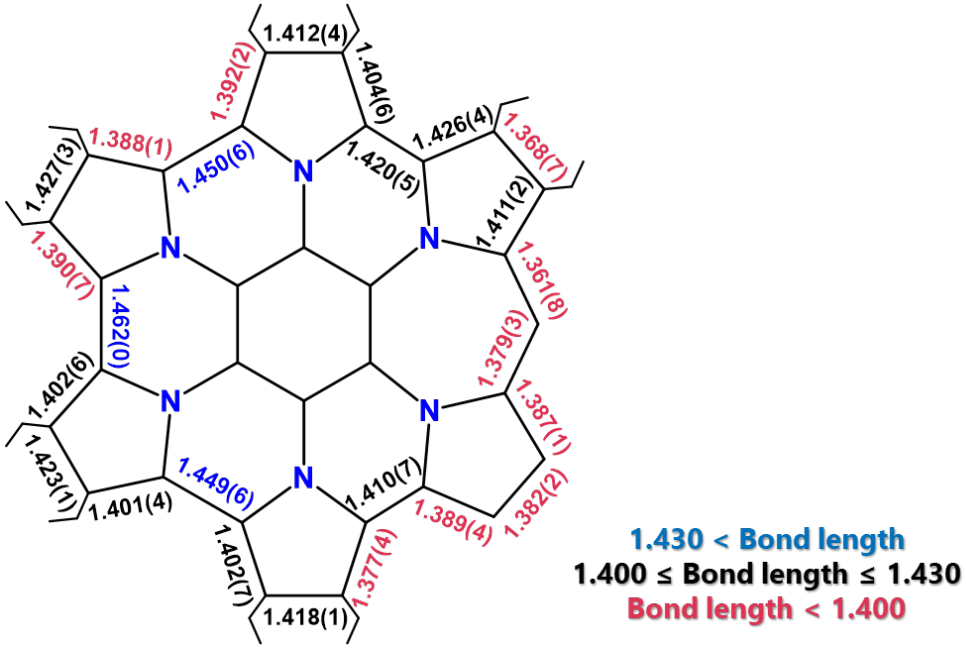

Figure S7. Selected bond lengths of the major disorder component of **3** from the single crystal analyses.

Table S7. Crystallographic refinement data for **3**.

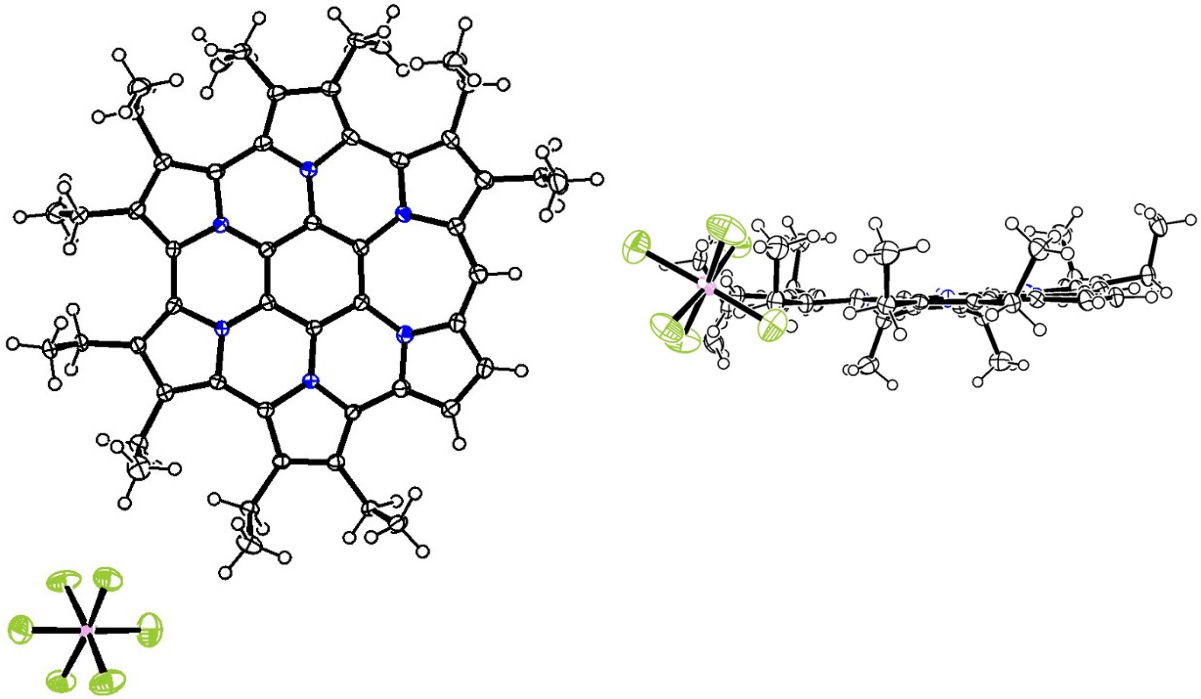

	3
Formula	$C_{51}H_{53}N_6$, SbF_6
Formula weight	985.74
Size	0.16 × 0.04 × 0.03
Radiation	Mo$K\alpha$
Temperature [K]	100
Crystal system	triclinic
Space group	*P*-1 (#2)
a [Å]	11.0231(5)
b [Å]	12.6110(4)
c [Å]	15.2281(4)
α [°]	98.437(2)
β [°]	93.659(3)
γ [°]	92.019(3)
V [Å^3]	2087.58(13)
Z	2
ρ [g·cm^{-3}]	1.568
μ [mm^{-1}]	0.734
F(000)	1012
No. of reflections measured	44460 (Total)
	11821 (Unique)
R_{int}	0.0621
R_1	0.0540
wR_2	0.1304
GOF	1.068
CCDC No.	2519098

S8. HOMA values

HOMA values of **1b**, **3**-Me and **3** were calculated using C–C and C–N bond lengths obtained from the X-ray crystallographic structures (for **1b** and **3**) and from optimised geometry (for **3**-Me) at B3LYP/6-31G(d) level of theory, according to the following equation; HOMA = $1-\alpha/n\Sigma\ (R_{opt} - R_i)^2$, where n is the number of bonds included in the summation, α is an empirical constant, R_{opt} is the optimal bond length, and R_i is the bond length of ith bond. The parameters R_{opt} = 1.388 Å (C–C) and 1.334 Å (C–N), and α = 257.7 (C–C) and 93.52 (C–N) were employed.[4]

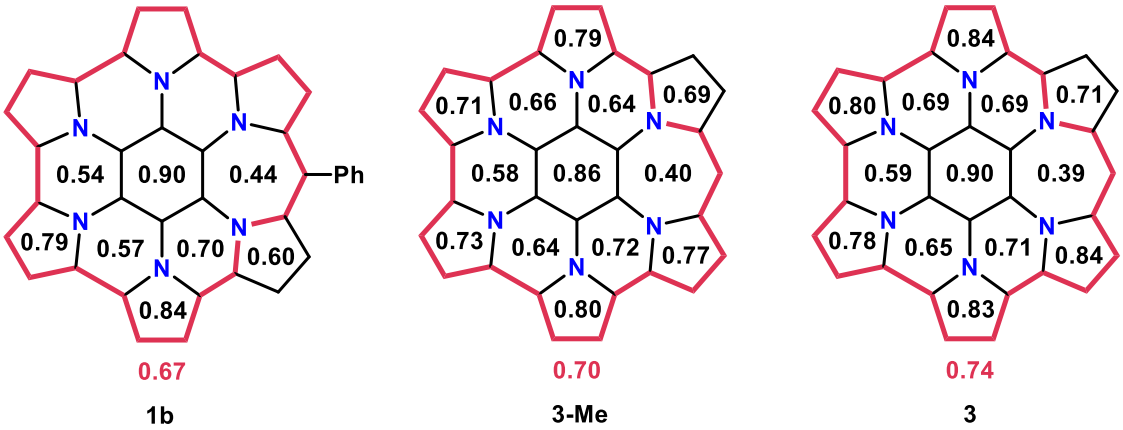

Figure S8. HOMA values of **1b**, **3**-Me, and **3**. The bonds used for HOMA calculations of the resonance structure are indicated in red lines.

S9. Cyclic voltammograms

Cyclic voltammetry (CV) of **1a** and **3** were measured under following conditions: 0.1 M $TBAPF_6$ in CH_2Cl_2, $Ag/AgNO_3$ reference electrode, Pt working electrode and Pt counter electrode, scan rate: 100 mV s^{-1}, potentials (vs Fc/Fc^+).

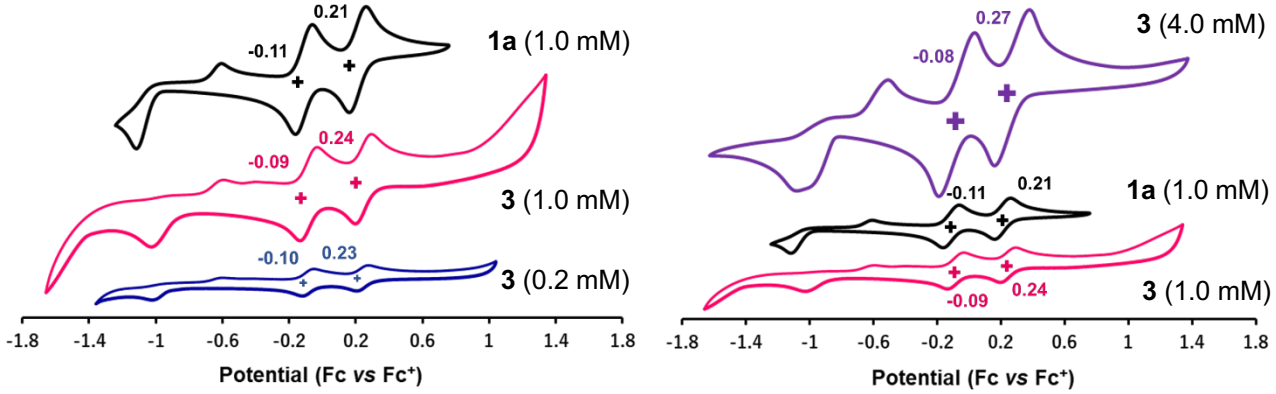

Figure S9. Cyclic voltammograms of **1a** (black line: 1.0 mM) and **3** (purple line: 4.0 mM, pink line: 1.0 mM, blue line: 0.2 mM).

S10. Absorption spectra

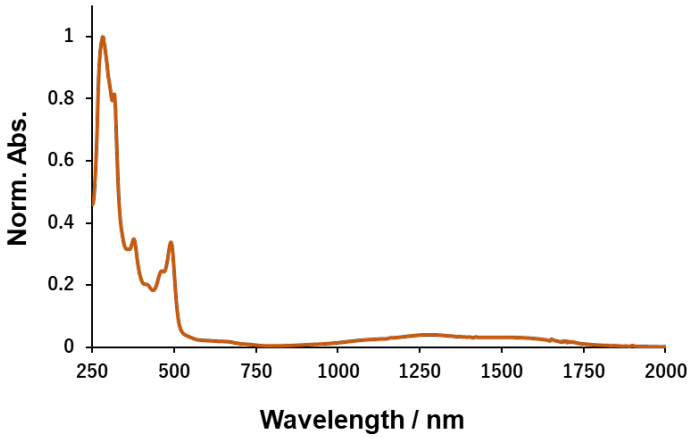

Figure S10a. UV-Vis-NIR spectrum of **3** in CH_2Cl_2.

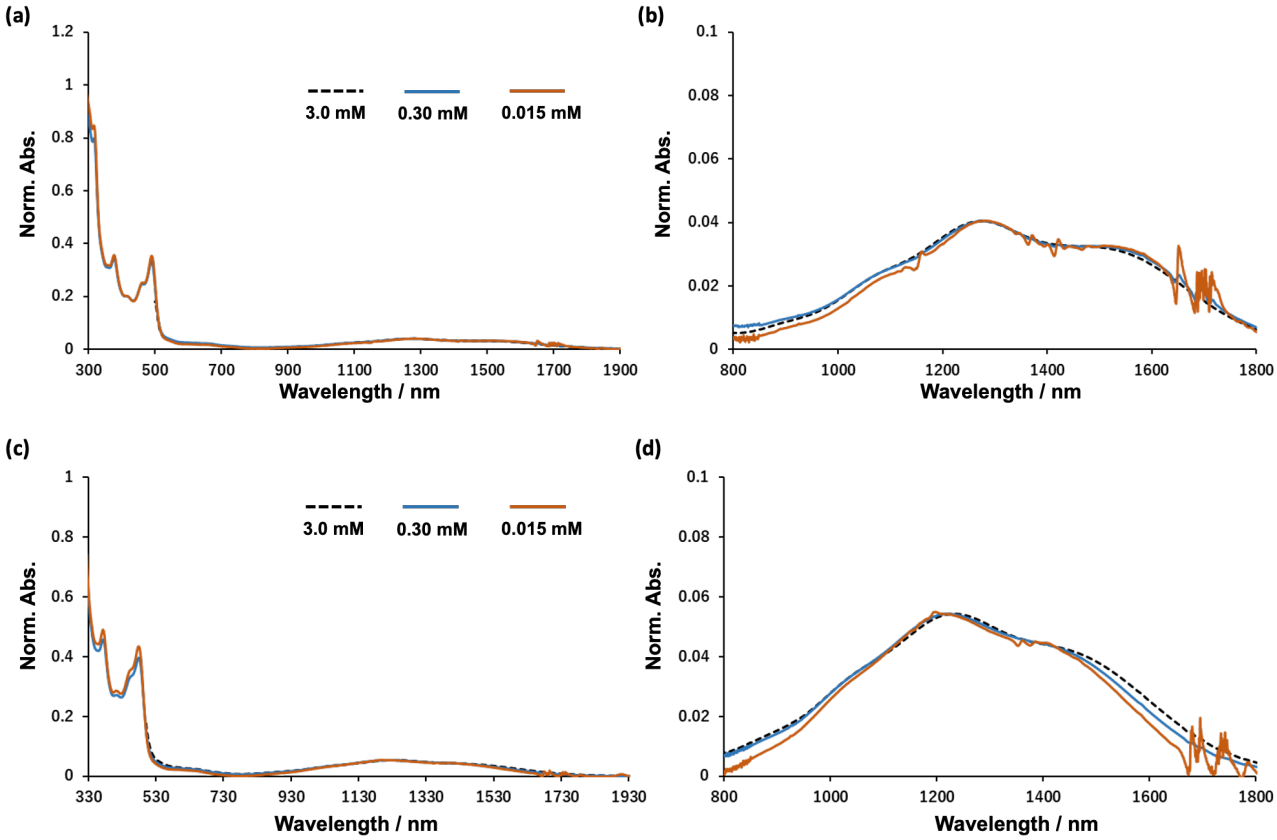

Figure S10b. UV-Vis-NIR spectra of **3** ([**3**] = 0.015, 0.30, and 3.0 mM) in CH_2Cl_2 (a,b) and acetone (c,d).

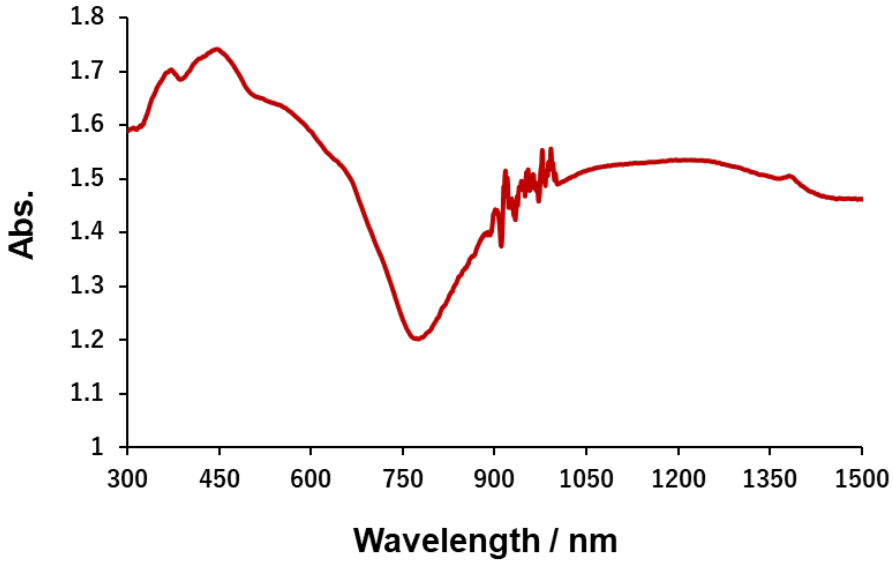

Figure S10c. Diffuse reflection UV-Vis-NIR spectrum of a solid sample of **3**.

S11. Molecular orbitals

All calculations were performed using the Gaussian 09 program package.[5] The initial geometries of the monomer and dimer of **3** were taken from their X-ray crystal structures. Visualisation of the results was performed using GaussView 5.0.

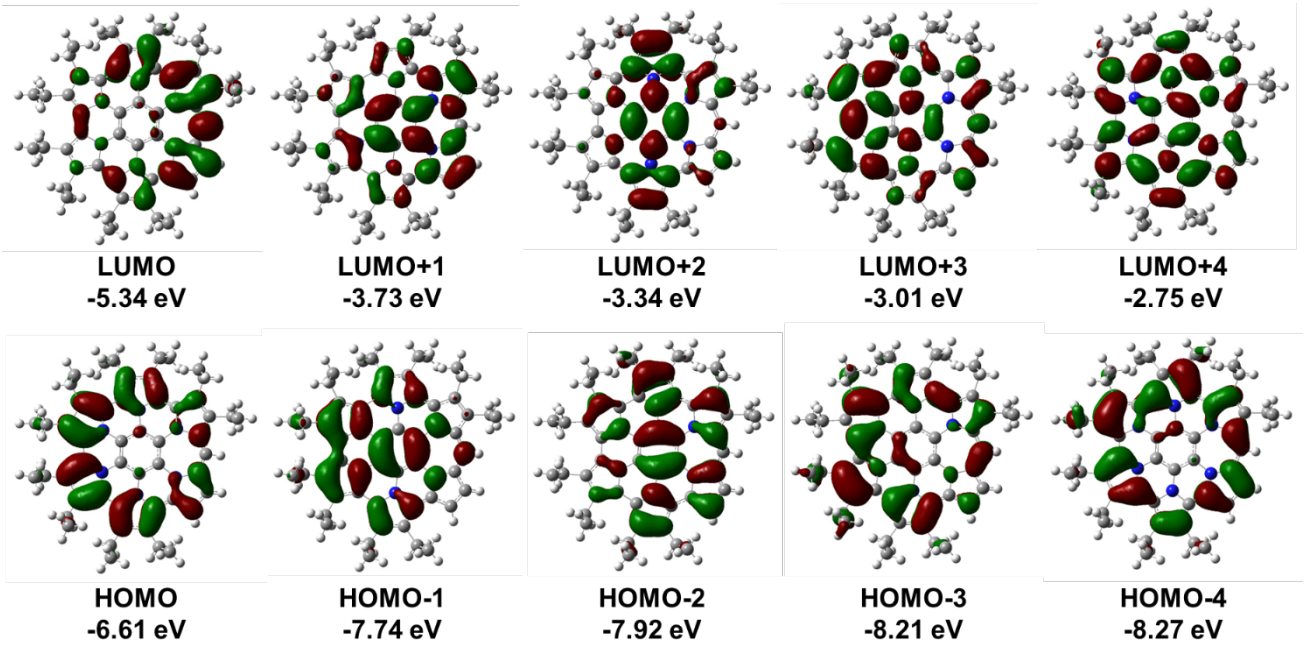

Figure S11a. Frontier molecular orbitals (isovalue = 0.02) and orbital energies of monomer **3** were calculated at the B3LYP/6-31G(d) level.

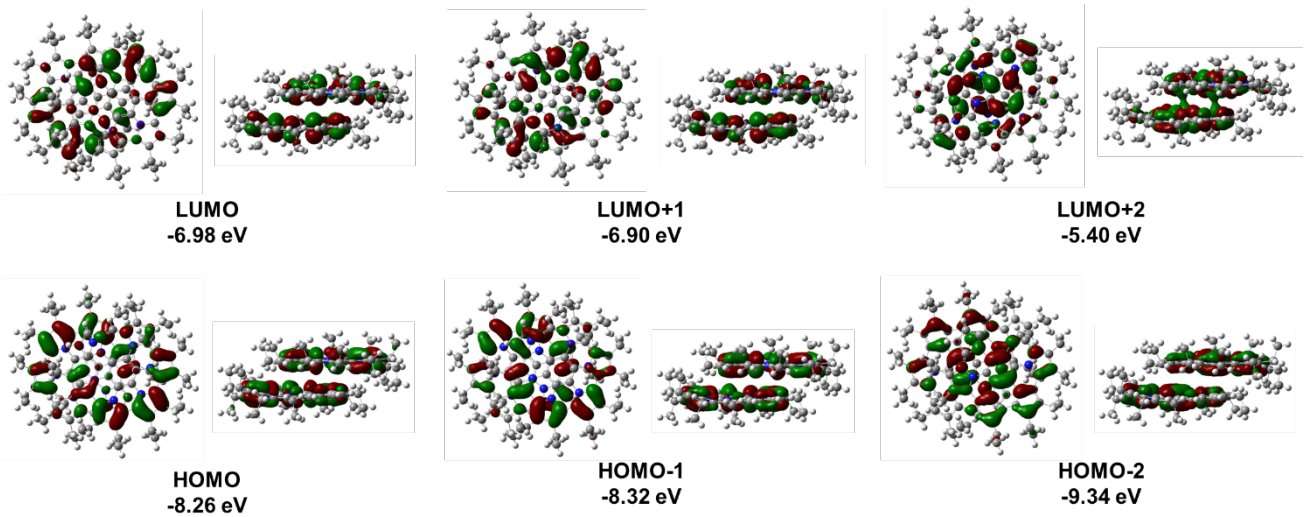

Figure S11b. Frontier molecular orbitals (isovalue = 0.02) and orbital energies of dimer **3** were calculated at the B3LYP/6-31G(d) level.

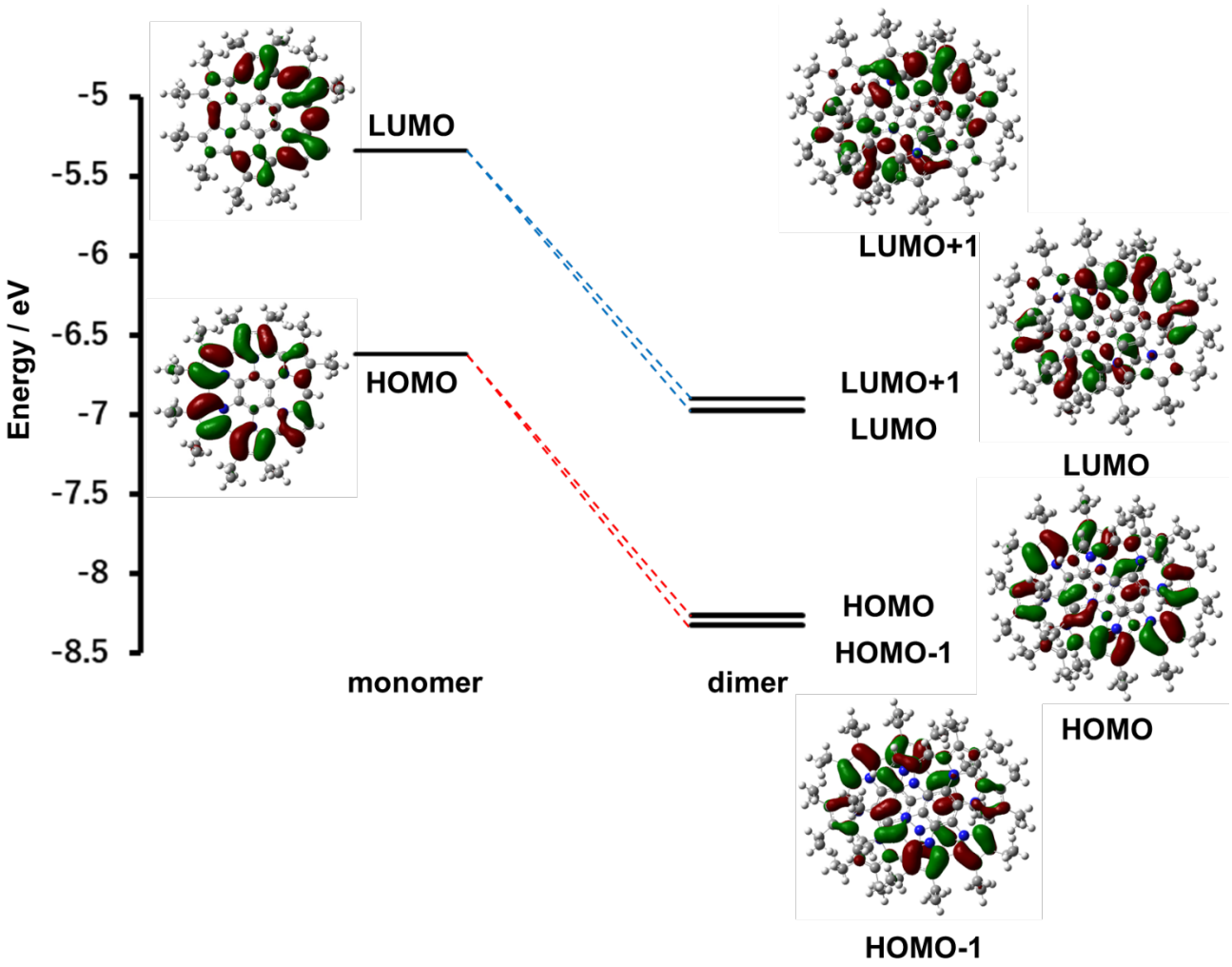

Figure S11c. Molecular orbital energy diagrams of monomer and dimer of **3**. The calculations were performed at the B3LYP/6-31G(d) level.

S12. TD-DFT calculations

All calculations were performed using the Gaussian 09 program package.[5] The geometries of the monomer and dimer of **3** were taken from their X-ray crystal structures. TD-DFT calculations were carried out at the B3LYP/6-31+G(d) level of the theory in the gas phase.

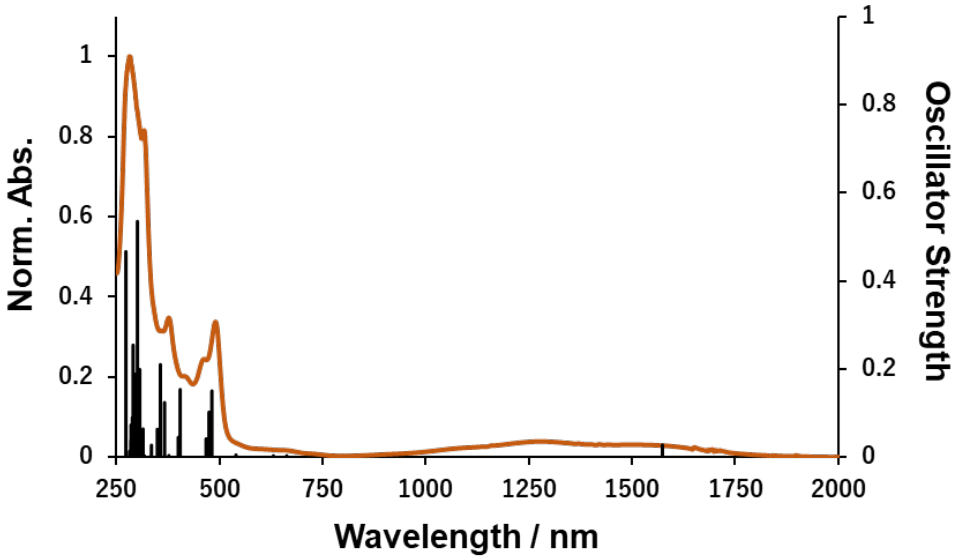

Figure S12a. UV-Vis-NIR spectrum of **3** in CH_2Cl_2 (spectrum, left axis) and corresponding TD-DFT results of monomer **3** (bar-graph, right axis).

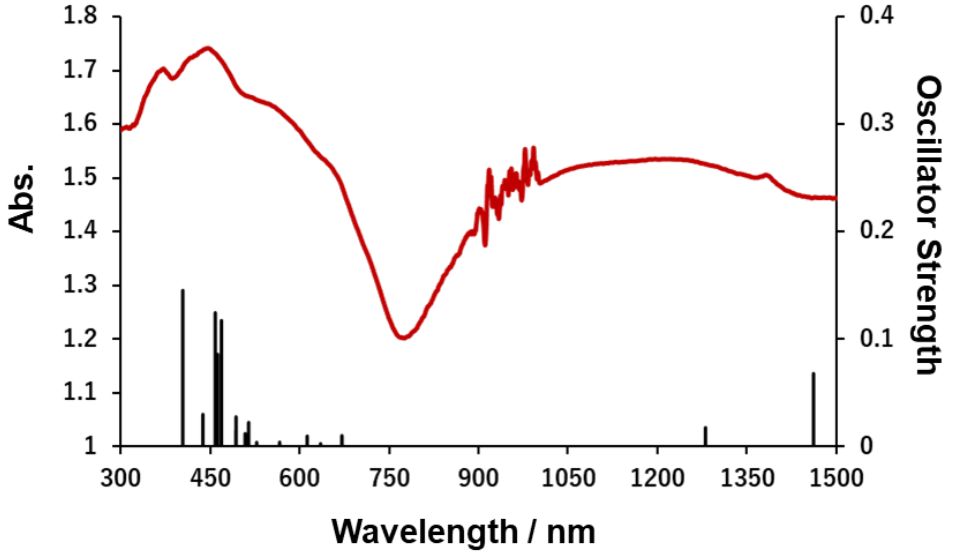

Figure S12b. Diffuse reflection UV-Vis-NIR spectrum of a solid sample of **3** (spectrum, left axis) and corresponding TD-DFT results of dimer **3** (bar-graph, right axis).

Monomer **3**

Excited State 1: Singlet-A 0.7878 eV 1573.79 nm f=0.0277 <S**2>=0.000
200 -> 201 0.70519
This state for optimization and/or second-order correction.
Total Energy, E(TD-HF/TD-DFT) = -2303.15727586
Copying the excited state density for this state as the 1-particle RhoCI density.

Excited State 2: Singlet-A 1.8701 eV 662.98 nm f=0.0034 <S**2>=0.000
199 -> 201 0.69473
Excited State 3: Singlet-A 1.9658 eV 630.71 nm f=0.0034 <S**2>=0.000
198 -> 201 0.69891
Excited State 4: Singlet-A 2.2959 eV 540.02 nm f=0.0051 <S**2>=0.000
200 -> 202 0.69872
Excited State 5: Singlet-A 2.5735 eV 481.77 nm f=0.1502 <S**2>=0.000
197 -> 201 0.67403
Excited State 6: Singlet-A 2.6123 eV 474.62 nm f=0.1023 <S**2>=0.000
196 -> 201 0.60422
200 -> 203 -0.30711
200 -> 204 -0.14681
Excited State 7: Singlet-A 2.6513 eV 467.64 nm f=0.0418 <S**2>=0.000
196 -> 201 0.27378
200 -> 203 0.62634
200 -> 204 -0.14881
Excited State 8: Singlet-A 3.0631 eV 404.77 nm f=0.1535 <S**2>=0.000
196 -> 201 0.14170
198 -> 203 -0.10232
199 -> 202 -0.31465
200 -> 204 0.59553
Excited State 9: Singlet-A 3.0977 eV 400.25 nm f=0.0452 <S**2>=0.000
194 -> 201 0.13055
195 -> 201 0.68275
Excited State 10: Singlet-A 3.2854 eV 377.38 nm f=0.0038 <S**2>=0.000
194 -> 201 0.68506
195 -> 201 -0.13692
Excited State 11: Singlet-A 3.3795 eV 366.87 nm f=0.1240 <S**2>=0.000
198 -> 202 0.26167
199 -> 203 -0.10233
200 -> 205 0.62107
Excited State 12: Singlet-A 3.4767 eV 356.62 nm f=0.2101 <S**2>=0.000
197 -> 202 0.14387
198 -> 203 -0.24607
199 -> 202 0.57257
200 -> 204 0.23212
Excited State 13: Singlet-A 3.5501 eV 349.25 nm f=0.0635 <S**2>=0.000
193 -> 201 -0.18352
198 -> 202 0.49762
199 -> 203 0.41370
199 -> 204 -0.13219
200 -> 205 -0.11886

Excited State 14:	Singlet-A	3.6992 eV	335.16 nm	f=0.0273	<S**2>=0.000
193 -> 201	0.66670				
199 -> 203	0.12866				
Excited State 15:	Singlet-A	3.7645 eV	329.35 nm	f=0.0002	<S**2>=0.000
200 -> 206	0.69065				
200 -> 208	-0.10650				
Excited State 16:	Singlet-A	3.8960 eV	318.23 nm	f=0.0030	<S**2>=0.000
197 -> 202	0.61909				
198 -> 203	0.27895				
Excited State 17:	Singlet-A	3.9403 eV	314.66 nm	f=0.0641	<S**2>=0.000
196 -> 202	0.56892				
197 -> 202	0.16415				
198 -> 202	-0.18431				
198 -> 203	-0.13948				
199 -> 203	0.24776				
Excited State 18:	Singlet-A	4.0440 eV	306.59 nm	f=0.1988	<S**2>=0.000
192 -> 201	-0.34015				
196 -> 202	0.21061				
196 -> 203	-0.10918				
197 -> 202	-0.12924				
198 -> 203	0.36861				
199 -> 202	0.12394				
199 -> 204	-0.19111				
200 -> 207	0.24044				
200 -> 208	0.10593				
Excited State 19:	Singlet-A	4.1050 eV	302.03 nm	f=0.0928	<S**2>=0.000
196 -> 202	-0.18789				
198 -> 202	-0.14510				
198 -> 203	0.16451				
199 -> 203	0.35879				
199 -> 204	0.45121				
200 -> 207	0.11499				
Excited State 20:	Singlet-A	4.1190 eV	301.01 nm	f=0.5349	<S**2>=0.000
190 -> 201	-0.11698				
192 -> 201	-0.20934				
196 -> 202	0.16927				
197 -> 203	-0.17389				
197 -> 204	0.12528				
198 -> 202	0.23594				
199 -> 203	-0.21774				
199 -> 204	0.41405				
200 -> 205	-0.18114				
Excited State 21:	Singlet-A	4.1920 eV	295.77 nm	f=0.1883	<S**2>=0.000
190 -> 201	0.10885				
192 -> 201	0.38597				
196 -> 202	0.13924				
196 -> 203	-0.12356				
197 -> 202	-0.14781				
197 -> 203	-0.23468				

198 -> 203 0.22817
199 -> 202 0.11056
199 -> 204 0.11135
199 -> 205 -0.24534
200 -> 207 -0.21716

Excited State 22: Singlet-A 4.2178 eV 293.96 nm f=0.0141 <S**2>=0.000
190 -> 201 0.19615
191 -> 201 -0.18617
192 -> 201 0.26829
195 -> 202 0.11026
196 -> 203 0.20103
197 -> 203 -0.11120
198 -> 204 0.15093
199 -> 205 0.20965
200 -> 207 0.43574

Excited State 23: Singlet-A 4.2682 eV 290.48 nm f=0.2543 <S**2>=0.000
191 -> 201 0.11537
192 -> 201 0.19192
197 -> 203 0.52778
198 -> 202 0.13454
199 -> 203 -0.14076
199 -> 205 -0.15671
200 -> 205 -0.10357

Excited State 24: Singlet-A 4.2820 eV 289.55 nm f=0.0068 <S**2>=0.000
190 -> 201 0.13771
191 -> 201 -0.11880
198 -> 204 0.14905
199 -> 205 0.17818
200 -> 206 0.11235
200 -> 207 -0.25297
200 -> 208 0.54727

Excited State 25: Singlet-A 4.2937 eV 288.76 nm f=0.0902 <S**2>=0.000
190 -> 201 -0.39040
196 -> 203 0.45513
197 -> 203 -0.12881
198 -> 204 0.16527
199 -> 205 -0.17401
200 -> 208 0.11956

Excited State 26: Singlet-A 4.3369 eV 285.88 nm f=0.0735 <S**2>=0.000
191 -> 201 0.53593
195 -> 202 0.13976
197 -> 203 -0.14777
198 -> 204 0.25673
199 -> 205 0.18696

Excited State 27: Singlet-A 4.3495 eV 285.05 nm f=0.0386 <S**2>=0.000
190 -> 201 -0.10888
191 -> 201 -0.29171
197 -> 203 0.10402
198 -> 204 0.41232

200 -> 207 -0.17991
200 -> 208 -0.27875
200 -> 209 0.24667
Excited State 28: Singlet-A 4.3636 eV 284.13 nm f=0.0104 <S**2>=0.000
190 -> 201 0.12568
196 -> 203 0.11995
198 -> 204 -0.15876
199 -> 205 -0.12536
200 -> 209 0.60932
Excited State 29: Singlet-A 4.3918 eV 282.31 nm f=0.0138 <S**2>=0.000
190 -> 201 0.37340
192 -> 201 -0.10145
195 -> 202 -0.25044
196 -> 203 0.15465
198 -> 204 0.30883
199 -> 205 -0.34322
200 -> 209 -0.11890
Excited State 30: Singlet-A 4.5392 eV 273.14 nm f=0.4664 <S**2>=0.000
190 -> 201 0.14017
196 -> 203 0.30463
197 -> 204 -0.29900
198 -> 203 0.18398
198 -> 204 -0.12777
198 -> 205 -0.16907
199 -> 205 0.22413
200 -> 207 -0.15137
200 -> 208 -0.14659
200 -> 210 0.12789
200 -> 211 0.17265
200 -> 213 -0.11542

Dimer **3**
Excited State 1: Singlet-A 0.8391 eV 1477.67 nm f=0.0000 <S**2>=0.000
399 -> 401 0.64856
400 -> 402 -0.27627
This state for optimization and/or second-order correction.
Total Energy, E(TD-HF/TD-DFT) = -4606.26643126
Copying the excited state density for this state as the 1-particle RhoCI density.

Excited State 2: Singlet-A 0.8484 eV 1461.44 nm f=0.0681 <S**2>=0.000
399 -> 402 -0.23199
400 -> 401 0.66517
Excited State 3: Singlet-A 0.8862 eV 1399.03 nm f=0.0000 <S**2>=0.000
399 -> 401 0.27619
400 -> 402 0.64915
Excited State 4: Singlet-A 0.9683 eV 1280.46 nm f=0.0178 <S**2>=0.000
399 -> 402 0.66631
400 -> 401 0.23343
Excited State 5: Singlet-A 1.8475 eV 671.08 nm f=0.0104 <S**2>=0.000

397 -> 402	0.11661				
398 -> 401	0.68840				
Excited State 6:	Singlet-A	1.9025 eV	651.70 nm	f=0.0000	<S**2>=0.000
397 -> 401	0.48565				
398 -> 402	0.49487				
Excited State 7:	Singlet-A	1.9392 eV	639.37 nm	f=0.0000	<S**2>=0.000
395 -> 401	0.18683				
396 -> 402	0.14683				
397 -> 401	-0.46191				
398 -> 402	0.47259				
Excited State 8:	Singlet-A	1.9520 eV	635.17 nm	f=0.0029	<S**2>=0.000
395 -> 402	0.22842				
396 -> 401	0.65060				
397 -> 402	-0.11720				
Excited State 9:	Singlet-A	2.0016 eV	619.42 nm	f=0.0000	<S**2>=0.000
395 -> 401	0.37038				
396 -> 402	0.55059				
397 -> 401	0.19537				
398 -> 402	-0.13200				
Excited State 10:	Singlet-A	2.0231 eV	612.85 nm	f=0.0099	<S**2>=0.000
396 -> 401	0.13291				
397 -> 402	0.67395				
398 -> 401	-0.11104				
Excited State 11:	Singlet-A	2.1470 eV	577.47 nm	f=0.0000	<S**2>=0.000
395 -> 401	0.56306				
396 -> 402	-0.40797				
Excited State 12:	Singlet-A	2.1881 eV	566.64 nm	f=0.0042	<S**2>=0.000
395 -> 402	0.66031				
396 -> 401	-0.23021				
Excited State 13:	Singlet-A	2.3253 eV	533.20 nm	f=0.0000	<S**2>=0.000
399 -> 404	-0.24867				
400 -> 403	0.65133				
Excited State 14:	Singlet-A	2.3474 eV	528.18 nm	f=0.0041	<S**2>=0.000
394 -> 402	0.12295				
399 -> 403	0.51590				
400 -> 404	-0.45906				
Excited State 15:	Singlet-A	2.3481 eV	528.01 nm	f=0.0000	<S**2>=0.000
391 -> 402	0.10857				
392 -> 401	-0.10868				
394 -> 401	0.66508				
400 -> 403	0.11634				
Excited State 16:	Singlet-A	2.4087 eV	514.74 nm	f=0.0226	<S**2>=0.000
391 -> 401	0.16627				
392 -> 402	-0.12840				
393 -> 401	0.16137				
394 -> 402	0.48536				
399 -> 403	0.21509				
400 -> 404	0.36910				
Excited State 17:	Singlet-A	2.4362 eV	508.93 nm	f=0.0123	<S**2>=0.000

391 -> 401 -0.11252
393 -> 401 -0.21965
394 -> 402 -0.33661
399 -> 403 0.41177
400 -> 404 0.38167

Excited State 18: Singlet-A 2.4465 eV 506.78 nm f=0.0000 <S**2>=0.000
394 -> 401 -0.10233
399 -> 404 0.64738
400 -> 403 0.23484

Excited State 19: Singlet-A 2.5050 eV 494.94 nm f=0.0000 <S**2>=0.000
392 -> 401 0.57640
393 -> 402 -0.36879
399 -> 404 0.10179

Excited State 20: Singlet-A 2.5125 eV 493.47 nm f=0.0278 <S**2>=0.000
391 -> 401 -0.13319
392 -> 402 -0.29658
393 -> 401 0.56152
394 -> 402 -0.25110

Excited State 21: Singlet-A 2.6148 eV 474.16 nm f=0.0000 <S**2>=0.000
392 -> 401 0.32937
393 -> 402 0.52462
399 -> 406 -0.11658
400 -> 405 0.26441
400 -> 407 -0.10335

Excited State 22: Singlet-A 2.6350 eV 470.52 nm f=0.0000 <S**2>=0.000
392 -> 401 -0.10137
393 -> 402 -0.25027
399 -> 406 -0.18485
400 -> 405 0.61053

Excited State 23: Singlet-A 2.6429 eV 469.13 nm f=0.1175 <S**2>=0.000
392 -> 402 0.48944
393 -> 401 0.23137
399 -> 405 -0.35701
399 -> 407 0.10363
400 -> 406 0.21586

Excited State 24: Singlet-A 2.6784 eV 462.91 nm f=0.0860 <S**2>=0.000
391 -> 401 0.15135
392 -> 402 0.33159
393 -> 401 0.16341
399 -> 405 0.49185
399 -> 407 0.12197
400 -> 406 -0.22420
400 -> 408 0.13459

Excited State 25: Singlet-A 2.7029 eV 458.71 nm f=0.1248 <S**2>=0.000
391 -> 401 0.62213
394 -> 402 -0.20401
400 -> 406 0.14321

Excited State 26: Singlet-A 2.7440 eV 451.85 nm f=0.0000 <S**2>=0.000
391 -> 402 0.68103

Excited State 27:	Singlet-A	2.8311 eV	437.94 nm	f=0.0301	<S**2>=0.000
399 -> 405	0.33316				
400 -> 406	0.60879				
Excited State 28:	Singlet-A	2.8592 eV	433.63 nm	f=0.0000	<S**2>=0.000
399 -> 406	0.66346				
400 -> 405	0.21789				
Excited State 29:	Singlet-A	3.0253 eV	409.82 nm	f=0.0000	<S**2>=0.000
397 -> 404	-0.12221				
398 -> 403	-0.17755				
399 -> 408	0.17673				
400 -> 407	0.62598				
Excited State 30:	Singlet-A	3.0663 eV	404.35 nm	f=0.1456	<S**2>=0.000
389 -> 402	-0.17474				
390 -> 401	0.37582				
397 -> 403	0.14865				
398 -> 404	0.16813				
399 -> 407	0.42561				
400 -> 408	0.24844				

S13. NICS and ACID calculations

Table S13. NICS(±1) values of monomer and dimer of **3** calculated at the GIAO/HF/6-311+G(d,p) level of the theory.

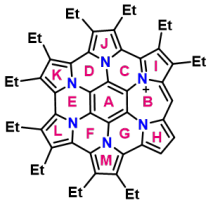

monomer

	NICS(1)	NICS(-1)
A	-5.4	-5.4
B	9.4	9.4
C	6.3	6.2
D	8.3	7.8
E	9.3	9.5
F	7.6	7.3
G	5.9	5.8
H	-4.0	-3.7
I	-2.7	-3.1
J	-7.8	-6.5
K	-6.3	-6.8
L	-6.3	-6.6
M	-7.2	-7.1

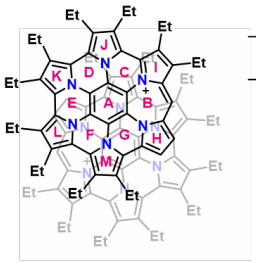

dimer

	NICS(1)	NICS(-1)
A	-5.8	-6.3
B	9.1	8.9
C	5.6	4.7
D	7.5	6.7
E	8.5	7.8
F	7.4	8.1
G	6.1	7.1
H	-3.8	-2.3
I	-2.9	-3.7
J	-7.9	-7.5
K	-6.8	-7.3
L	-6.5	-8.1
M	-6.6	-6.0

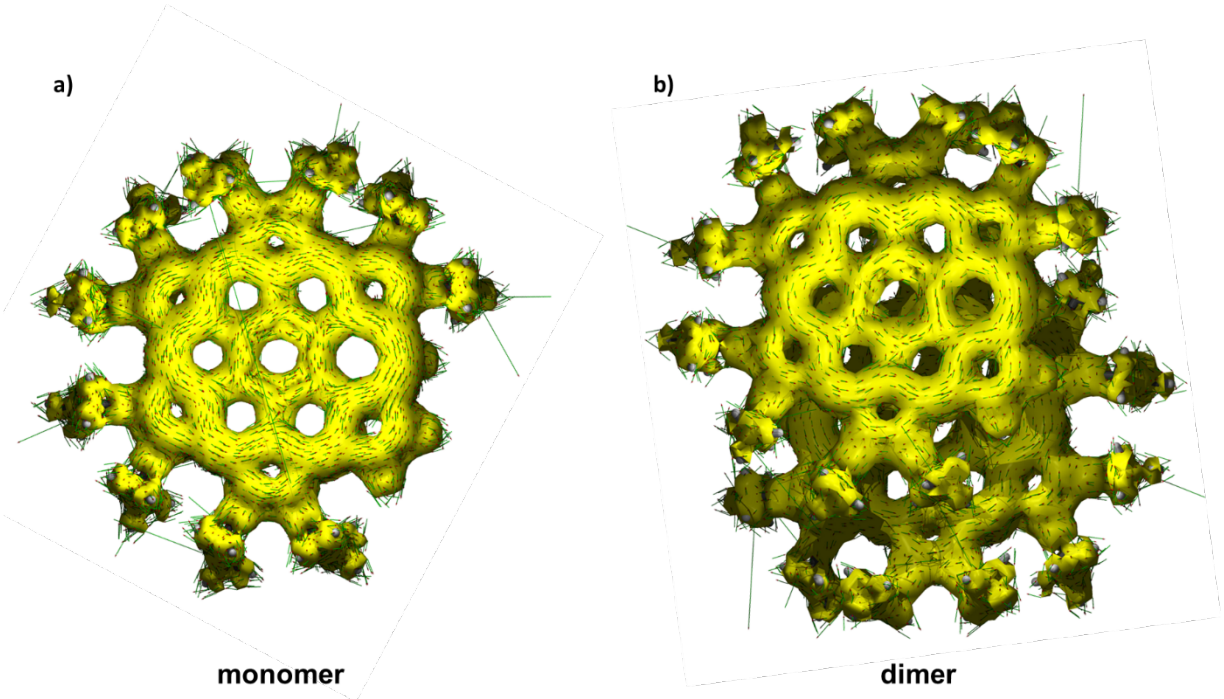

Figure S13. ACID plots of (a) monomer and (b) dimer of **3** were calculated at CSGT/B3LYP/6-31+G(d). For ACID calculations, the magnetic field is perpendicular to the molecular center and points out through the paper. Isovalue is 0.03.

S14. Atomic coordinates of optimized structure

Atomic coordinates of the optimised structure of **3**-Me calculated at the B3LYP/6-31G(d) level of theory are provided. Ethyl groups were replaced with methyl groups to simplify the calculations. Frequency calculations were carried out to confirm that their structures correspond to local minima on the potential energy surface.

3-Me

C	-1.04184	0.38318	-0.10772	C	-1.07292	-0.94988	-0.09289	C	0.08099	-1.61936	0.01595
C	1.28785	-0.99957	0.11496	C	1.31693	0.36788	0.11905	C	0.13378	1.02376	-0.00383
N	0.05108	2.29569	-0.0293	N	-2.14734	1.00236	-0.21865	N	-2.19005	-1.5524	-0.18643
N	-0.05664	-2.88584	0.02628	N	2.28813	-1.79751	0.13559	N	2.3463	1.13664	0.21033
C	1.08259	3.03727	0.05948	C	0.62618	4.30506	0.04322	C	-0.70473	4.24835	-0.149
C	-1.04514	2.94849	-0.14395	C	-3.27705	0.41351	-0.31968	C	-4.18316	1.40056	-0.4402
C	-3.51857	2.56912	-0.33468	C	-2.20876	2.27487	-0.23519	C	-2.28929	-2.8245	-0.17594
C	-3.60175	-3.08502	-0.31212	C	-4.24194	-1.89831	-0.3384	C	-3.30274	-0.93504	-0.29319
C	-1.15398	-3.53823	-0.04414	C	-0.83092	-4.84397	0.06766	C	0.51094	-4.91675	0.16942
C	0.94538	-3.64915	0.14754	C	3.50166	-1.56552	0.42519	C	4.19326	-2.70351	0.60827
C	3.30594	-3.68812	0.48256	C	2.14368	-3.06441	0.24527	C	2.27865	2.42556	0.16443
C	3.52423	2.94041	0.21869	C	4.34925	1.90478	0.40521	C	3.57204	0.81105	0.37223
C	-1.55321	5.4698	-0.36007	C	1.32858	5.61461	0.26849	C	5.84542	1.96707	0.59166
C	4.04589	4.33592	0.03673	C	1.34384	-6.16474	0.26946	C	-1.72334	-6.0481	0.15667
C	-5.7391	-1.77859	-0.35879	C	-4.30413	-4.40364	-0.46652	C	-4.21712	3.89842	-0.29197
C	-5.66113	1.31719	-0.69517	C	4.13241	-0.394	0.50707	H	5.25718	-2.82538	0.85056
H	3.52316	-4.75061	0.62313	H	-0.97028	6.32279	-0.76984	H	-2.29993	5.29702	-1.16093
H	-2.01919	5.81304	0.58985	H	2.10322	5.52396	1.05537	H	1.7154	6.05186	-0.67809
H	0.65273	6.37317	0.71986	H	6.21814	2.98801	0.81931	H	6.17179	1.3597	1.46507
H	6.36665	1.60605	-0.32388	H	3.4749	4.87853	-0.74229	H	4.11246	4.88589	1.00091
H	5.0668	4.33905	-0.40233	H	0.7842	-7.08887	0.01375	H	2.17864	-6.13619	-0.46537
H	1.74795	-6.28367	1.30001	H	-2.01222	-6.41133	-0.85431	H	-1.23957	-6.89723	0.68444
H	-2.60653	-5.83887	0.79394	H	-6.24068	-2.67754	0.05979	H	-6.08033	-0.97701	0.32717
H	-6.12102	-1.63775	-1.39406	H	-3.71952	-5.08929	-1.11283	H	-4.53696	-4.85784	0.52198
H	-5.26088	-4.30802	-1.02393	H	-5.26593	3.81297	0.06512	H	-3.76619	4.5585	0.47601
H	-4.24852	4.37552	-1.29636	H	-5.88949	0.52034	-1.43147	H	-6.23062	1.19086	0.25206
H	-6.05465	2.22425	-1.20239	H	5.21693	-0.45596	0.69589				

S15. References

[1] J. -S. Chen and R. B. Shirts, *J. Phys*. *Chem*., 1985, **89**, 1643.

[2] *SHELXT*: G. M. Sheldrick, *Acta Crystallogr*., 2014, **A70**, C1437.

[3] *SHELXL*: G. M. Sheldrick, *Acta Crystallogr.*, 2008, **A78**, 112.

[4] *HOMA*: T. M. Krygowski and M. K. Cyrański, *Chem. Rev*. 2001, **101**, 1385.

[5] Gaussian 09, Revision D.01, M. J. Frisch,

G. W. Trucks, H. B. Schlegel, G. E. Scuseria, M. A. Robb, J. R. Cheeseman, J. A. Montgomery, Jr., T. Vreven, K. N. Kudin, J. C. Burant, J. M. Millam, S. S. Iyengar, J. Tomasi, V. Barone, B. Mennucci, M. Cossi, G. Scalmani, N. Rega, G. A. Petersson, H. Nakatsuji, M. Hada, M. Ehara, K. Toyota, R. Fukuda, J. Hasegawa, M. Ishida, T. Nakajima, Y. Honda, O. Kitao, H. Nakai, M. Klene, X. Li, J. E. Knox, H. P. Hratchian, J. B. Cross, V. Bakken, C. Adamo, J. Jaramillo, R. Gomperts, R. E. Stratmann, O. Yazyev, A. J. Austin, R. Cammi, C. Pomelli, J. W. Ochterski, P. Y. Ayala, K. Morokuma, G. A. Voth, P. Salvador, J. J. Dannenberg, V. G. Zakrzewski, S. Dapprich, A. D. Daniels, M. C. Strain, O. Farkas, D. K. Malick, A. D. Rabuck, K. Raghavachari, J. B. Foresman, J. V. Ortiz, Q. Cui, A. G. Baboul, S. Clifford, J. Cioslowski, B. B. Stefanov, G. Liu, A. Liashenko, P. Piskorz, I. Komaromi, R. L. Martin, D. J. Fox, T. Keith, M. A. Al-Laham, C. Y. Peng, A. Nanayakkara, M. Challacombe, P. M. W. Gill, B. Johnson, W. Chen, M. W. Wong, C. Gonzalez, and J. A. Pople, Gaussian, Inc., Wallingford CT, 2013.